AD-A224 585

FIRST SEMIANNUAL REPORT

for period

15 January 1990 through 15 July 1990

AUTOMATED HANDLING AND ASSEMBLING OF NON-RIGID ~~RIDGE~~ OBJECTS

for

OFFICE OF NAVAL RESEARCH

on

Contract No. N-00014-90-J-1516

by

Yuan F. Zheng, Principal Investigator
Dept. of Electrical Engineering
The Ohio State University
Columbus, OH 43210

TABLE OF CONTENTS

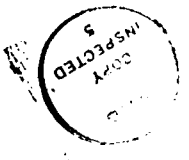

STATEMENT "A";Correct title should read:
"Automated Handling and Assembling of Non Rigid Objects" per Cdr. J. Sheridan
ONR/Code 11D
TELECON 7/23/90 VG

1. INTRODUCTION

The goal of this research project is to investigate the mechanisms for automated handling and assembling of non-rigid objects. This is to be accomplished by approaching four aspects of the problem:

a. Study the deformation characteristics of non-rigid materials.

b. Investigate optimal tool structure for handling non-rigid objects.

c. Develop the sensing mechanism to locate non-rigid objects.

d. Develop the motion control mechanism for the host machines.

This semiannual report summarizes the results of the research achieved during the period January 15, 1990 through July 15, 1990. In this period, two topics have been studied. The first topic addresses the strategies of automated assembling of non-deformation objects. The study takes a typical assembly task, inserting a flexible beam into a rigid hole, as the target of study. Assembly mechanism have been developed for both loose clearance and tight clearance cases. In the loose clearance case, it is found that the deformed beam curve is the best tool trajectory for assembly. In the tight clearance case, however, the tool trajectory needs to be modified in order to eliminate the effect of the resistance force. The involute of the beam curve is found to be the optimal trajectory of modification.

The second topic is the identification of deformation characteristics and estimation of object deformation by using vision sensors. To automatically handle and assemble deformable objects, a key point is to understand the deformation behavior of the objects. Mathematical descriptions of the object deformation has been found very complicated. In addition, deformation characteristics of the objects in many cases are unknown. This makes impossible even to have a mathematical description. The goal of this study is to find the deformation characteristics by using a vision sensor. Once the deformation characteristics is defined the deformation behavior can further be studied by mathematical analysis, or alternatively by using vision system again to measure the deflection of the object.

The study in this period has been concentrated on one-dimensional objects. In the next period, we plan to continue the research on one-dimensional objects and to extend the research

to two-dimensional objects including the sensor identification of the deformation behavior, and optimal tool structure and assembly mechanisms for handling both types of objects.

The rest of this report presents the results of the two research topics as just summarized as well as the research plan for the next period.

2. AUTOMATIC ASSEMBLY OF ONE-DIMENSIONAL OBJECTS

Deformable objects may be one, two or three-dimensional. Our investigation starts from one-dimensional objects since the latter is the most fundamental among the three, and the results can be further extended to two and three-dimensional objects. To study the mechanism of automatic assembly of one-dimensional objects, we also take a typical assembly task, inserting a deformable peg (flexible beam) into a rigid hole as the target of study (Fig. 1). The peg insertion task has been studied by Whitney and Simunovic of Charles Stark Draper Laboratory and other scientists (see Appendix A). Many fundamental issues of assembly are included in the peg insertion tasks. It is considered that if the mechanisms can be successfully developed for the peg-insertion task, mechanisms for other assembly tasks can be likewise developed.

In investigating the beam insertion mechanism, we first study the behavior of beam deformation. From earlier studies, it is known that the position and orientation of the peg end-must precisely match the hole. For deformable objects, the position and orientation of the tool is not the same as that of the free end which goes into the hole. As a result, we must first investigate the deformation behavior of a flexible beam such that the tool trajectory can be found based on the required position and orientation of the beam end. We use Rhode's method to describe the beam deformation. In this method, the deformation is described by the Mclaurin's series since there does not exist a closed-form solution for the deformation (for the series description, see next section of this report).

In developing the assembly mechanism, we first reviewed the conditions of assembly for rigid objects. It is found that the conditions proposed for rigid parts by Whitney are also applicable to flexible beams. Since the latter are flexible as a whole, but their surfaces that

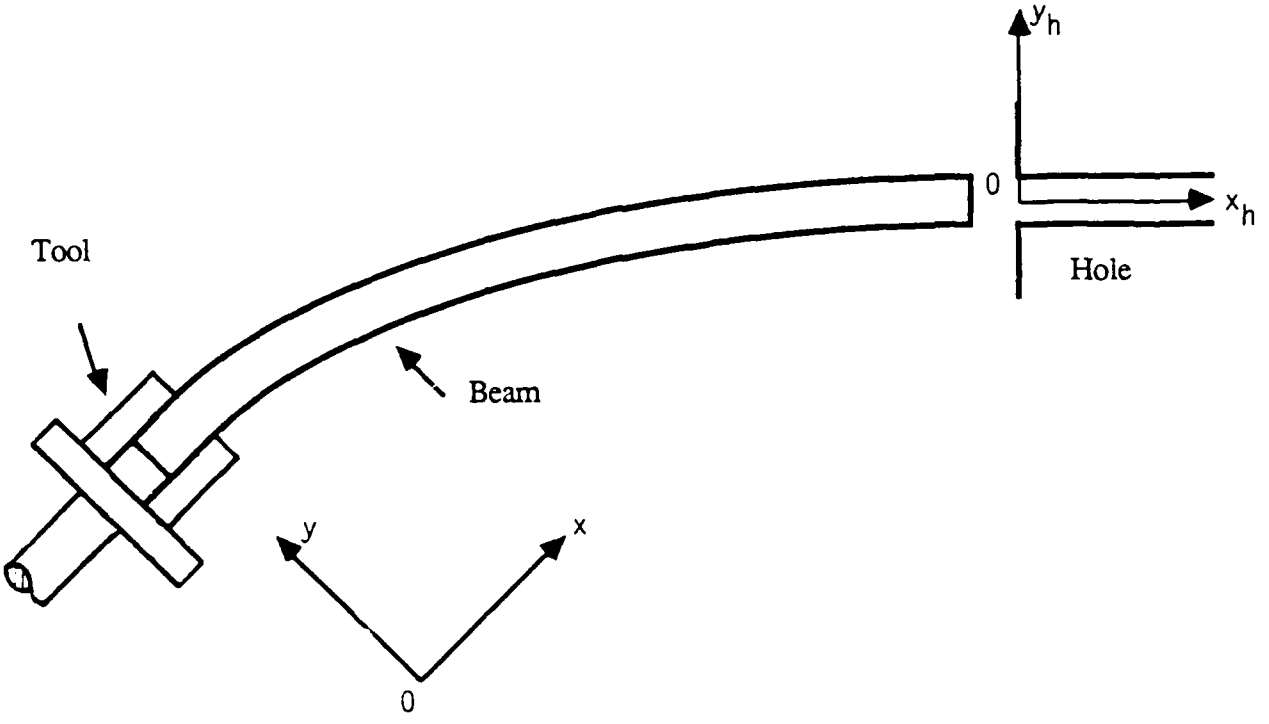

Fig. 1 A deflected beam is to be inserted into a hole

make contact with the inner-surface of the hole are still rigid. As a result, the geometric and force conditions for successful assembly of rigid objects are still valid for deformable beams.

Base on the deformation behavior of the beams and the assembly conditions, we have developed assembly mechanisms for both loose and tight clearance assembly. Loose clearance means that the difference between the radius of the beam and that of the hole is relatively large; therefore, the beam does not experience large resistance when it is inserted into the hole. Tight clearance indicates that the difference is very small, and the beam encounters large resistance force when it is inserted.

For the loose clearance case, it is found that the best trajectory of assembly for the tool is the curve formed by contour of the deformed beam. When the tool follows the contour of the deformed beam, the beam is naturally deflected by its own weight, and no force is interacted between the beam and the hole. Consequently, one of the assembly conditions, minimizing the interaction force between the hole and the beam, is best satisfied, and assembly is more likely to be successful. For tight clearance case, if the tool trajectory is still the same as in the loose clearance case, the interaction force between the hole and the beam must be increased to counterbalance the resistance force. This violates the assembly conditions. We propose to modify the tool trajectory following the involute of the naturally-deflected beam curve. The total deflection of the beam is reduced to reflect the effect of the resistance force. Thus, the reaction force between the hole and the beam is minimized again.

The assembly mechanisms proposed for both the loose and tight clearance cases are verified by experiments in our laboratory. In both experiments, successful results have been achieved.

A technical paper has been written based on the results just described. The details of the assembly mechanisms can be found in the paper which is attached to this document as Appendix A, "Strategies for Automatic Assembly of Deformable Objects."

3. VISION IDENTIFICATION OF DEFORMATION BEHAVIOR OF ONE-DIMENSIONAL OBJECTS

For one-dimensional objects, deflection can be described by the following equation

$$EI\frac{1}{\rho} = EI\frac{d\theta}{ds} = M(s). \tag{1}$$

where ρ is the radius of curvature, E is the stiffness of the material, I is the moment of inertia of the cross-sectional area, s is the length of the beam, θ is the tangential angle at point s which is called deflection angle in our research, and M(s) is the deflection moment exerting at point s. Since M(s) is a nonlinear function of s, (1) is difficult to solve. Take the derivative of (1) with respect to s, one obtains the following equation

$$\frac{d^2\theta}{ds^2} = \frac{\omega}{EI} s\cos\theta \tag{2}$$

where ω is the weight density of the beam. From (2), it can be seen that the deformation behavior is determined by the term $\frac{\omega}{EI}$. We therefore call it the deformation characteristic. For a one-dimensional object, it is difficult to identify its deformable characteristic by using its fundamental parameters, since ω, E and I are not feasible to obtain in reality. We propose to use vision sensors for the identification purpose. The procedures for small deflection can be briefly described as follows.

Using Maclaurin's series method, the solution of (2) can be expressed as

$$\theta(s) = \theta(0) + \theta'(0)s + \frac{1}{2!}\theta''(0)s^2 + \cdots\cdots . \tag{3}$$

By using the boundary conditions of the beam, (3) can be expressed as

$$\theta_l = \theta_0 - \frac{1}{6}\cos(\theta_0)(\frac{\omega}{EI})\, s^3 - \frac{1}{180}\sin(\theta_0)\,(\frac{\omega}{EI})^2\cos(\theta_0) - \frac{1}{8640}\cos^3(\theta_0)(\frac{\omega}{EI})^3 s^9$$
$$- \frac{1}{12960}\sin^2(\theta_0)\cos(\theta_0)(\frac{\omega}{EI})^3 s^9 + \cdots . \tag{4}$$

where θ_0 is the deflection angle of the beam end and θ_l is the angle of the gripper which holds the other end of the beam. θ_l is known from the gripper orientation, and θ_0 is measured from the vision sensor. Once the two angles are known, $\frac{\omega}{EI}$ can be precisely solved from (4).

After the deformation characteristic is defined, the deformation behavior of a deformable object can be calculated. Basically, during the assembly process, the required orientation and position of the beam end is given. The problem is to find what should be the orientation and position of the gripper which holds the other end of the beam (Fig. 1). We using a numerical method with the assistance of the vision sensor. First the length of the beam curve l is divided equally into n small segments, each with a length h. Then, by using the Lagrangian interpolation formula, equation (2) can be expressed as

$$\theta_{i+2} - 2\theta_{i+1} + \theta_i = h^2(\frac{-\omega}{EI})s_{i+1} \cos(\theta_{i+1}), \tag{5}$$

where θ_i denote $\theta(s_i)$ and $s_i = ih$ for $i = 0, 1, 2, ...n$. To start the computation of (5), one needs θ_0 and θ_1. θ_0 is measured by using the vision sensor, θ_1, however, can be obtained from the Lagrangian quadratic interpolation of $\theta'(s_0)$ which is

$$\theta'(s_0) = (2h)^{-1}(-\theta_2+4\theta_1-3\theta_0). \tag{6}$$

Since $\theta'(s_0) = \theta'(0) = 0$ and $\theta(s_0) = \theta_0$, it turns out that

$$\theta_1 = \frac{1}{4}\theta_2 + \frac{3}{4}\theta_0. \tag{7}$$

Substitute θ_1 in (5) by (7), one obtains

$$\theta_2 = \theta_0 - 2h^3 (\frac{\omega}{EI}) \cos(\frac{1}{4}\theta_2 + \frac{3}{4}\theta_0). \tag{8}$$

θ_2 can be easily solved from (8). After θ_2 is known, θ_1 can be calculated by (7). Iteration can thus be started. After all the θ_i's are obtained, the positions of the each knot point (x_i, y_i) can be calculated as

$$x_i = \sum_i h \cos(\theta_i), \text{ and } y_i = \sum_i h \sin(\theta_i). \quad (9)$$

The attached paper Appendix B, "Deformation Identification and Estimation of One-Dimensional Objects by Vision Sensors," further presents the details of the method just described.

3. RESEARCH PLAN FOR THE NEXT SEMIANNUAL PERIOD

In the next period, we plan to continue our research on one-dimensional objects, and at the same time start to study the automated handling and assembling of two dimensional objects. For one-dimensional objects, we will investigate optimal tool structures which are the best in handling objects with large deformations, and in mating flexible peg and hole with large resistance forces. At this point, we consider to use multiple end-effectors to handle flexible objects. For this, coordination between multiple end-effectors will be investigated.

For two-dimensional objects, we will first study the deformation characteristics. Then the identification of the deformation behavior by using vision sensors will be investigated again. Based on the identified deformation, mechanism including the tool structure for handling the objects and the motion trajectories of the tool will be studied.

APPENDIX A

STRATEGIES FOR AUTOMATIC ASSEMBLY OF DEFORMABLE OBJECTS

Yuan F. Zheng, Run Pei and Chichyang Chen
Dept. of Electrical Engineering
The Ohio State University
Columbus, OH 43210

ABSTRACT

Strategies for automatic assembly of deformable objects are presented in this paper. A flexible beam mating with a rigid hole is taken as the target of investigation. First, the deflection behavior of a deformable beam is studied. Then the geometric and force conditions for successfully assembly of rigid parts are reviewed. Based on these conditions of assembly, strategies for assembling deformable beams are proposed. The strategies are defined by the motion trajectory of the tool which handles the beam. It is found that when the clearance between the beam and the hole is loose, the desired trajectory should be the same as the curve formed by the deformed beam. When the clearance is tight, position and orientation of the tool should be adjusted, following the involute of the deformed beam curve. Experimental results are finally given to prove that the proposed strategies are effective.

ACKNOWLEDGEMENT: This work is supported by the Office of Naval Research under grant N0014-90-J-1516. Part of Yuan Zheng's work is also supported by the Presidential Young Investigator Award from the National Science Foundation (grant DDM-8996238).

1. INTRODUCTION

Automated handling and assembling of materials have been studied by many experts in the areas of manufacturing, robotics, and artificial intelligence. Until now, most studies have assumed that the objects to be manipulated are rigid; but, in reality, there is a frequency occurrence of non-rigid objects. For example, in the shipbuilding, aerospace and automobile industries, flexible plates are widely used for assembling various vehicles. In the electronics industry, a single printed-wiring-board (PWB) consists of up to 24 flexible inner layers printed with delicate wires. In fact, even rigid objects tend to become deformable when the object's dimension become extensive.

The automated handling and assembling of non-rigid objects is hindered by their essential characteristics including: low elasticity, large deformation caused by external forces and momentums, complicated dynamic behavior, and large physical dimension. As a result, automated handling and assembling of non-rigid objects have never been seriously addressed. In most cases, non-rigid materials and parts are still handled and assembled by human hands. For example, the inner layers contained in a PWB are assembled together by human hands, where layer upon layer of flexible pieces are added to a base plate until a "book" is assembled. The book is then laminated to form a PWB. The assembly of PWBs by human beings not only is inefficient but also results in many errors because the printed inner layers need to be precisely aligned; and the ability of humans to achieve this level of precision varies from operator to operator [1].

Since the handling and assembling of non-rigid objects is involved in a wide range of manufacturing applications, the automated handling and assembling of such objects become critically important to improve manufacturing efficiency and product quality. Unfortunately, in reviewing the available literature, we only found a few works which studied the automation of handling non-rigid objects; and in many cases, only ad hoc methods were proposed. For example, in Europe, Petry

and Bick designed a cell for the automated insertion of insulating mats into the interior of automobiles [2]. The insulating mats were flat and soft; and, traditionally they had been inserted by humans. Petry and Bick designed special tools to pick up the mats and used robots to insert them into automobiles. Although the designed cell was reported successful, the proposed methods were limited to a special application. General knowledge of handling non-rigid objects was not presented.

Another issue related to automated handling of non-rigid objects is the recent research on flexible manipulators. Compared with rigid arms, flexible manipulators are light weight and hence easily maneuverable. However, because of the arm deformation and vibration induced by the joint motion, modeling and control of flexible arms is considered difficult. Nevertheless, a considerable amount of work has been published on the subject such as references [3-5]. Unfortunately, all those studies only consider how to control the flexible machines, not the flexible objects. The latter does not have actuators, and is not feasible to install any sensor on. Consequently, the methods developed for controlling flexible manipulators are not applicable to flexible objects.

In general, deformable objects may be one-dimensional such as a flexible beam, two-dimensional such as a flexible plate, or three-dimensional such as a deformable body. The study of this paper will concentrate on one-dimensional objects, since the latter are the most fundamental among the three. The results, however, can be extended to two and three-dimensional objects. Also, the typical assembly task, inserting a deformable peg (beam) into a rigid hole, is taken as the target of study. The peg insertion task for rigid objects has been extensively studied by other scientists ([6, 7]). It is considered that if good mechanisms can be found for the peg insertion task, methods for assembling of other type objects can be accordingly derived.

The structure of the paper is as follows. In the next section, we first study the behavior of beam deformation. The purpose is to identify the deformed shape of flexible beams. It is known that an assembly may fail if the position and

orientation of the peg end do not match the same of the hole [6]. For deformable object, the trajectory of the tool which handles the beam is no longer the same as the free end of the beam, but must comply with the deflected shape. An adequate trajectory can be found only when the deformed shape is identified.

In the third section, the conditions for a successful assembly of rigid parts as presented in [6] and [7] will be reviewed. Although deformable beams are not rigid as a whole, the surface of the object which makes the contact with the hole are still rigid; therefore, the same conditions should be applicable to deformable beams.

In the fourth section, assembly mechanisms for the loose clearance is first investigated. The mechanism is defined by the required trajectory of the tool. Two criteria are chosen to select the trajectory. The first criterion is that the selected trajectory should guarantee a successful insertion of the beam following the conditions of assembly as presented in the previous section. The second criterion is that the selected trajectory should result in a minimum motion of the tool such that the assembly consumes the minimum energy. Based on the two criteria, the best trajectory is found to be the curve formed by the deflected beam.

In the fifth section, study is concentrated on the tight clearance case. When the clearance between the beam and the hole is tight, the beam experiences large resistance force during the insertion. In order to overcome the resistance force, the tool trajectory must be modified. It is found that the involute of the beam curve is an effective trajectory of modification.

In the sixth section, experiments of beam assembly for both loose and tight clearance cases are presented. The experimental results prove that the mechanism proposed in this paper are effective for assembling of deformed objects. Finally, conclusions are presented in the seventh section.

2. DESCRIPTION OF BEAM DEFLECTION

Consider that a beam-structured object is grasped by the tool of an automated machine (robot end-effector, for example). Since the object is non-rigid, the beam is deflected under the influence of its own weight (Fig. 1). The position and orientation of the beam's free-end is no longer a simple transformation from the other end held by the tool. To understand the relation between the two ends, the deflection behavior of the beam must be known.

From classical mechanics, it is well known that the deflection of a beam can be described by the following equation ([8]):

$$EI\frac{1}{\rho} = EI\frac{d\theta}{ds} = M(s) \qquad (1)$$

where ρ is the radius of curvature, E the stiffness of the material, I the moment of inertia of the cross-sectional area, s the length of the beam from the origin, and M(s) the deflecting moment exerting at point s of the beam. Since M(s) in (1) has a non-linear relation with s, solving (1) is not an easy issue. Classical mechanics and applied mathematics have provided many solutions. Here, we use Rhode's method as presented in [9].

For convenience, we assume the origin of the beam to be at the free-end of the beam. Equation (1) can be turned into:

$$EI\frac{d\theta^2}{ds^2} = -\omega s \cos\theta \qquad (2)$$

where ω is weight density of the beam. Assume that the deflection angle at the free-end of the beam is given as θ_0. The boundary conditions of (2) are $\theta(0) = \theta_0$, and $d\theta(0)/ds = 0$ (no deflecting moment exerts at the free-end). There does not exist a closed form solution to (2). Instead, the solution is expressed in terms of a series:

$$\theta = \sum_{n=0}^{\infty} a_n s^n. \tag{3}$$

From (3), one may get

$$\frac{d\theta}{ds} = \sum_{n=1}^{\infty} n a_n s^{n-1} \tag{4}$$

and

$$\frac{d^2\theta}{ds^2} = \sum_{n=2}^{\infty} n(n-1) a_n s^{n-2} \tag{5}$$

By using the boundary conditions and expanding both sides of (2), one may get ([9]):

$$a_0 = \theta(0) = \theta_0,$$

$$a_1 = \frac{d\theta(0)}{ds} = 0,$$

$$a_2 = \frac{d^2\theta(0)}{2!ds^2} = -\frac{1}{EI}\omega\, s \cos\theta(s)|_{s=0} = 0,$$

$$a_3 = \frac{d^3\theta(0)}{3!ds^3} = -\frac{\omega}{EI}[\cos\theta(s) - s \sin\theta(s)\, \theta'(s)]\, |_{s=0} = -\frac{\omega}{EI}\cos\theta_0,$$

$$a_6 = \frac{a_3\omega}{30EI}\sin\theta_0, \text{ and } a_{3n+4} = a_{3n+5} = 0,\ n = 0, 1, 2 \ldots, \text{ etc.}$$

As a result, the deflection angle can be expressed as:

$$\theta(s) = \theta_0 + \sum_{k=1}^{\infty} a_{3k}\, s^{3k}. \tag{6}$$

By using (6), one may also find the deflected position of point s in the (x,y) coordinates. Since $dy/ds = \sin\theta$, one has

$$y(s) = \int_0^s \sin\theta(t)dt = A_1(s)\sin\theta_0 + A_2(s)\cos\theta_0 \qquad (7)$$

where $A_1(s) = s - (a_3)^2 s^7/14 - a_3a_6s^{10}/10 - \cdots$, and $A_2(s) = a_3s^4/4 + a_6s^7/7 + [a_9-(a_3)^3/6]s^{10}/10 + \cdots$. Likewise, one may have

$$x(s) = A_1(s)\cos\theta_0 - A_2(s)\sin\theta_0. \qquad (8)$$

Equations (6), (7) and (8) give a general description of the beam deflection. If the deflection is small, (6), (7) and (8) can be simplified by using their first approximation [9], i.e.:

$$\theta(s) = \theta_0 + a_3s^3, \qquad (9)$$

$$y(s) = s\sin\theta_0 + a_3 s^4 \cos\theta_0/4 \qquad (10)$$

and

$$x(s) = s\cos\theta_0 - a_3 s^4 \sin\theta_0/4. \qquad (11)$$

If the deflection is small, and the deflection angle at the free-end is expressed as:

$$\theta_0 = \frac{\omega L^3}{6EI} \qquad (12)$$

one may have the maximum deflection of y at y = L being

$$y(L) = s\sin\theta_0 + a_3s^4\cos\theta_0/4 = \frac{\omega L^4}{8EI} \qquad (13)$$

The results of (12) and (13) are in agreement with small deflection theory of many textbooks dealing with material mechanics ([8], [10]).

From the above discussion, it can be seen that the deflection behavior and the mathematical descriptions of the behavior are very complicated unless the deflection is small. In the rest of this paper, however, our assembly mechanism is based on a known deflection. The deflection beha ior can be obtained by a numerical computation based on (9), (10) and (11) if the deflection is small. Or (6), (7) and (8) when the deflection is large. Even when (6), (7) and (8) are used, solutions are still approximate since it is impossible to compute all the terms in the series. However, more precise solutions can be obtained by including more terms in the computation. On the other hand, if parameters E, I or ω are not given, one will not be able to use those formulations. Instead, the deflection can only be measured in reality. Vision is probably the best mechanism to use for this purpose. Using a vision system to measure the deflection of a beam has also been studied. The result is reported in another paper ([10]) and will not be discussed here.

3. CONDITIONS FOR SUCCESSFUL ASSEMBLY

Assembly of rigid parts was previously studied by many works such as [6],[7] and [12]. It was pointed in [6] and [7] that for rigid parts, assembly is a geometric problem. In order to successfully complete the assembly, theoretical and experimental studies have revealed certain conditions that must be met while positioning the parts and applying insertion force on the parts. For the peg insertion task, Whitney summarized the following three conditions [7].

(1) The peg must first cross the chamfer such that the insertion to the hole could start. For this, the following condition must be met:

$$|e_0| < w \tag{14}$$

where e_0 is the initial position error of the peg and w is the width of the chamfer as shown in Fig. 2a.

(2) One reason for the failure of the peg-insertion is wedging. Wedging makes the peg got stuck in the hole. The cause of wedging is geometric rather than applied forces [6]. To avoid wedging, the insertion angle q must meet the following condition when two-point contact occurs (Fig. 2b):

$$|q| < c/\mu \tag{15}$$

where c = (R-r)/R called clearance ratio, and μ is the coefficient of friction; R and r are the radius of the hole and the peg respectively.

(3) Another reason for the failure of the peg-insertion is jamming. Jamming is a condition that the applied forces and moments applied to the peg are in a wrong proportion. To avoid jamming, the following inequalities must be satisfied:

$$|M/rF_x + \mu(1+\lambda)F_y/F_x| < \lambda \tag{16}$$

and

$$|F_y/F_x| < 1/\mu \tag{17}$$

where $\lambda = l/2r\mu$ with l being the length of the part which has been inserted in the hole, and M, F_x and F_y are the applied moment and forces as shown in Fig. 2b. Note that here F_x is aligned with the axis of the peg and F_y is perpendicular to the axis.

The above three conditions reveal that in order to successfully complete the insertion task, first, the tip of the peg must be precisely positioned to the hole (at least cross the chamfer) before the insertion starts. Secondly, the direction of the insertion should be closely aligned with the axis of the hole, i.e., the insertion angle should be very small. Finally, the applied force in the insertion direction F_x should be large, but the one in the lateral direction F_y and the applied moment M should be as small as possible.

We consider that the same conditions are still applicable to the assembly of deformable beams. Although the beam is not rigid as a whole, deformation occurs only along the main axis of the beam. The surface of the beam which contacts with

the hole is still rigid. Consequently, the geometric and force relations between the surface of the beam and hole must still satisfy the above three conditions. However, the interactions between the beam and the hole are controlled by the tool which holds the other end of the deflected beam. Then the question becomes what should be the behavior of the tool such that the geometric and force relations satisfy the above three conditions?

It could be noticed that two issues are involved in the mating of rigid parts. One is the position and orientation of the tool and the other is the force and moment applied by the tool. For deformable beams, however, only the position and orientation of the tool need to be considered. This is because the beam is deformable, and the end of the beam which is held by the tool still has three degrees of freedom even when a portion of the beam is inside the hole. That is, no position constraints are imposed on the tool. As a result, the tool is not able to control the force and moment in the direction which the tool has no motion freedom. Thus, one is not able to directly control the interaction forces between the beam and the hole. Instead, the latter can only be controlled by properly positioning the tool.

4. ASSEMBLY MECHANISM FOR LOOSE CLEARANCE

In this section, we study the tool trajectory for the loose clearance case, i.e., the difference between the radius of the beam and the hole is relatively large, and the resistance that the hole imposes on the beam is small. In the next section, we will further consider the tight clearance assembly. Note that in this paper, the hole is assumed to be rigid and straight.

Consider a deformable beam with a length of L that needs to be inserted into a hole whose axis has an angle of θ_0 with the x axis of the world coordinates (Fig. 1). For convenience, we attach a coordinate frame (x_h, y_h) to the hole, with the x_h axis aligned with the axis of the hole and the original point at the entrance of the hole (Fig. 1). To find an optimal trajectory, we divide the assembly procedure into three phases, *approaching phase*, *initial insertion phase* and *insertion phase*. For

each phase, the details need to be further discussed. The following definitions, however, are for convenience in our discussion.

Definition 1 Any point of the beam which coincides with the original point of the (x_h, y_h) coordinates during the assembly process is called the end of the beam (note that the terminal point of the beam which goes into the hole is called the free-end of the beam).

Definition 2 The tangent vector at the end of the beam is called the end tangent vector. The one at the free-end is called the free-end tangent vector.

Definition 3 The curve that describes the shape of a deformed beam which is outside the hole is called the beam curve.

A. Approaching Phase

In this phase, the tool brings the beam to approach and finally make a contact to the hole. To successfully complete the assembly, the free-end of beam must be precisely positioned and orientated before the insertion starts such that the first two conditions as summarized in the previous section are satisfied. It is clear that when the contact is made, the position of the free-end should be at the original point of the (x_h, y_h) coordinates and the orientation should be aligned with the x_h axis. The position and orientation of the tool, however, should not be the same as the free-end of the beam, but must be specified according to the deflection of the beam. From our earlier discussion, it can be seen that the position and the orientation of the tool in the (x_h, y_h) coordinates should be:

$$\begin{vmatrix} p_x \\ p_y \\ \theta \end{vmatrix} = \begin{vmatrix} -A_1(L) \\ A_2(L) \\ \sum_{k=1}^{\infty} a_{3k} L^{3k} \end{vmatrix} \tag{18}$$

for large deflections, and

$$\begin{vmatrix} p_x \\ p_y \\ \theta \end{vmatrix} = \begin{vmatrix} -L \\ \frac{\omega L^4}{8EI} \\ \frac{\omega L^3}{6EI} \end{vmatrix} \tag{19}$$

for small deflections. Note that (18) and (19) represent a rotational transformation of (6)-(11) from the (x, y) coordinates to the (x_h, y_h) coordinates. Once the tool moves to the point as specified by (18) or (19), the free-end of the beam makes a contact to the hole. Next, the initial insertion process can start.

B. Initial Insertion Phase

The purpose of this phase is to insert a small portion of the beam into the hole such that the hole can start to apply forces to the beam or vice versa. The length of this small portion depends on the total length and the weight of the beam and should be selected in reality. In general, it should be long enough such that the beam can apply the force to the hole without loosing the contact. On the other hand, it should not be too long such that the deflection of the beam caused by its own weight is distorted. The reason for the later limitation will be made clear as our study proceeds.

Assume the length of the small portion is ΔL. To insert the portion into the hole, the tool should be moved to the following point

$$\begin{vmatrix} p_x \\ p_y \\ \theta \end{vmatrix} = \begin{vmatrix} -A_1(L) + \Delta L \\ A_2(L) \\ \sum_{k=1}^{\infty} a_{3k} L^{3k} \end{vmatrix} \tag{20}$$

for large deflections, and

$$\begin{vmatrix} p_x \\ p_y \\ \theta \end{vmatrix} = \begin{vmatrix} -L + \Delta L \\ \frac{\omega L^4}{8EI} \\ \frac{\omega L^3}{6EI} \end{vmatrix} \tag{21}$$

for small deflections. This completes the initial insertion phase.

C. Insertion Phase

From the description of the initial insertion phase, it is clear that as a small portion is inserted into the hole, the end tangent vector is no longer aligned with the x_h axis. The discrepancy becomes bigger as the tool moves further. As a result, the second condition as specified in the previous section will be violated. Then the question is: how can we maintain the orientation of the end tangent vector always aligned with the axis of the hole, and at the same time the reaction force between the hole and the beam is minimum ? Before answering this question, we need to make following proposition.

Proposition 1 The minimum force that the hole exerts on the beam is the force that counterbalances the weight of the portion which is inside the hole.

Proof: It is mentioned earlier that the hole is straight; therefore, the portion of the beam that is inside the hole has no deflection. Recall that the deflection is caused by the weight of the beam. Since the beam has no deflection inside the hole, the deflection effect of the weight must be counterbalanced by the force exerted on the beam by the hole.

It was mentioned in the previous section that in order to have a smooth assembly, the force that the hole exerts on the beam in the y_h direction should be as small as possible. From the proposition just proved, it is known that the minimum force should at least counterbalance the weight of the portion which is inside the hole. It follows that if we can maintain the minimum force as the beam is inserted into the hole, the assembly is in its best condition.

Since the resistance force is very small, and the reaction force from the hole only counterbalances the weight of portion which is inside the hole, the force exerted on the outside portion is negligible. As a result, the portion outside the hole can be considered as free beam with its free-end being at the original point of the (x_h, y_h) coordinates. Consequently, to maintain a minimum reaction force between the beam and the hole, the tool should follow such a trajectory that the outside portion of the beam always behaves as a free beam (virtual free beam), and its end tangent vector is always aligned with the x axis of the hole. This kind of motion continues until the beam is completely inserted into the hole. Any other trajectory will result in a large reaction force, and the assembly is more likely to fail.

It appears that we have to continuously find the beam deflections as the beam length changes. This is apparently not feasible in practical applications. After a careful study of the deflection behavior, however, we find that the desired tool trajectory follows a well defined pattern.

Claim 1 The desired trajectory of the tool for an optimal hole insertion should follow the beam curve which appears at the end of the approaching phase.

Proof: At the end of the approaching phase, the beam is completely outside the hole. From equation (1), it is known that the curvature of any point on the beam is

determined by the weight of its right-side portion of the beam (the portion with the free-end) and has nothing to do with the left portion of the beam. As a result, the beam curve of a beam with a length of s (Fig. 3a) is the same as the portion of a longer beam if the portion has the same length of s from the end (Fig. 3b). Thus, the shape of the beam curve when the beam first contacts the hole defines the beam curves of all the virtual free beams before the beam is completely inserted into the hole. It follows that the trajectory of the tool is the same as the beam curve when the approaching phase is just completed. ♦

By using the claim just proved, it is easy to specify the trajectory of the tool. Actually, once the deflection of the beam is found by using (6), (7) and (8), or by (9), (10) and (11), the assembly trajectory of the tool is simultaneously defined. Assume that the insertion speed is determined to be ds/dt = V. One can drive the required motion speed of the tool from the (6), (7) and (8) as:

$$\frac{dy}{dt} = \frac{dA_2(s)}{ds} V, \tag{22}$$

$$\frac{dx}{dt} = \frac{dA_1(s)}{ds} V \tag{23}$$

and

$$\frac{d\theta}{dt} = V \sum_{k=1}^{\infty} a_{3k} s^{3k-1}. \tag{24}$$

Again, the tool velocities expressed in (22), (23) and (24) are expressed in the (x_h, y_h) coordinates. Also in reality, only a few terms in (22)-(24) can be evaluated.

5. MECHANISM FOR TIGHT CLEARANCE ASSEMBLY

The three phases as employed in the loose clearance case can still be used here. The approaching and initial insertion phases are identically in both cases. The

insertion phase, however, needs to be modified. In this section, we first discuss why the insertion needs to be modified, and then the modification procedure is identified.

A. The Effect of the Resistance Force

The resistance force is aligned with the end tangent vector of the beam (Fig. 4), and generates deflecting moment on the beam. When the resistance force or the beam deformation is very small, the deflecting moment is negligible. When the clearance becomes tight, or the deflection of the beam is large, the effect of the resistance force cannot be ignored.

If the same trajectory as in the loose clearance case is still employed, the moment generated by the resistance force must be compensated by additional force and moment exerted by the hole in order to maintain a free beam status (Fig. 4). The latter force and moment not only violate the third condition of assembly as previously discussed, but also make the friction force even larger. As a result, the assembly becomes more difficult to success.

From Fig. 4, it can be seen that the moment generated by the resistance force actually counteract the moment generated by the weight of the beam. The deflection of the beam should become smaller with the resistance force if no additional force and moment are to be exerted by the hole. Consequently, one should reduce the deflection in order to successfully complete the assembly.

B. Tool Trajectory for Tight Clearance Assembly

Essentially, the tool should move to a new position and orientation which leads the beam to a smaller deflection. It appears that the simplest method is to fully extend the beam such that the beam has no deflection (Fig. 5). However, there are two problems with this strategy.

First, when the beam has no distortion, the resistance force has no deflecting effect on the beam. But the deflecting effect by the weight of the beam is still there which is actually counterbalanced by the additional force and moment exerted by the

hole. The latter force and moment again violate the third condition of assembly. The second problem is that the distance that the tool travels in making the insertion is increased. Recall that in the loose clearance case, the insertion follows the shape of the beam curve. The distance that the tool travels is the same as the length of the beam L. To make the beam fully extended, the tool has to move from the original position as specified by (18) or (19) along a special curve AB to point (L, 0) before the insertion starts (Fig. 5). The total distance travelled becomes $L + L_a$ where L_a is the length of curve AB. This prolonged length makes the assembly less energy-efficient. In order to have an efficient assembly, the tool should make as small an adjustment as possible, and at the same time the total deformation is reduced enough to offset the effect of the resistance force. Basically, the beam curve should have a shape between fully extended and fully deflected as shown in Fig. 5.

Finding the right curve for AB turns out to be a difficult issue. If the curve is not adequately selected, the assembly may fail again. For example, the tool could be moved too much away from the hole, and the free-end of the beam loses its contact with the hole (Fig. 6a). On the other hand, the tool could be too close to the hole, the deflection becomes worse (Fig. 6b). One method to find the right trajectory of the tool is to solve the fundamental deflection equation with the resistance force added, i.e., turning (2) into the following equation:

$$EI\frac{d\theta^2}{ds^2} = -\omega s \cos\theta + F \sin(\theta_0 - \theta). \qquad (25)$$

where F denotes the resistance force. Theoretically, one may find x, y and θ at s=L by solving (25). The computation involved, however, is substantial. The unknown resistance force F makes the situation even worse.

A simple solution is proposed for this problem. First, the deflecting effect of the resistance force is very small to the portion which is close to the end of the beam since the force is tangential to the end. One may simply consider that the curvature of that portion is not affected by the resistance force. Second, the effect to the portion which is close to the tool-end, is very significant, and its curvature is

greatly reduced by the resistance force. A simple consideration is that the curvature becomes zero, and as the resistance force increases, the length of the zero-curvature portion becomes longer. In the maximum case, the beam should be fully extended to totally eliminate the effect of the resistance force. Based on this intuitive analysis, we propose the following curve as AB.

Claim 2 If the tool moves along the involute of the beam curve, which appears when the beam first contacts the hole (at the end of the approaching phase), and the orientation of the tool is perpendicular to the tangent of the involute, the tool and the hole can spend a curve with the total length being the original length of the beam, and the orientation difference between the hole and the tool becomes smaller. In addition, the curve is very close to the beam curve which is under the influence of the resistance force and its own weight.

Proof: Without losing generality, we can assume the curve which describes the shape of the free beam to be a unit speed curve (a curve $\alpha(t)$: t -- R^2 is a unit speed curve if $|d\alpha(t)/dt| = 1$ [13]) and denoted as $\alpha(s)$. The involute of $\alpha(s)$ can be described as ([13]):

$$\beta(s) = \alpha(s) + (L-s)\, T(s) \tag{26}$$

where $T(s) = \alpha'(s)$. If the tool is at point $\beta(t_0)$ of the involute, one curve that could be spanned by the tool and the hole is the portion of curve $\alpha(s)$ from 0 to t_0 plus the straight line between $\alpha(t_0)$ and $\beta(t_0)$. The total length of this curve is :

$$\begin{aligned} \text{Total Length} &= \int_0^{t_0} d\alpha(s) + (L-t_0) \\ &= \int_0^{t_0} dt + L - t_0 \\ &= t_0 + L - t_0 = L \end{aligned} \tag{27}$$

which is the same as the length of the beam (Fig. 7). The orientation of the tool at point $\beta(t_0)$ is orthogonal to the tangent of $\beta(s)$ at t_0, which is $\mathbf{T}(t_0)$ since the tangent of $\beta(s)$ is $\beta'(s)$, and

$$\begin{aligned}[\mathbf{T}(s)]^T \beta'(s) &= [\mathbf{T}(s)]^T [\alpha'(s) + (L-s)\,\mathbf{T}'(s) - \mathbf{T}(s)] \\ &= [\mathbf{T}(s)]^T[\mathbf{T}(s) + (L-s)\,\mathbf{T}'(s) - \mathbf{T}(s)] \\ &= [\mathbf{T}(s)]^T\,\mathbf{T}'(s)(L-s) \\ &= 0. \end{aligned} \tag{28}$$

$\mathbf{T}(t_0)$, however, represents the tangent vector of curve $\alpha(t_0)$ at point t_0. As a result, the orientation difference between the hole and the tool becomes smaller.

Next we need to prove that the curve just described is very close to the beam curve under the influence of the resistance force. In [14] it is described that the involute can be formed by manipulating a string using the following steps. First, take a string of length L, fasten one end at the end of the beam for which s=0 and bring the string into coincidence with the beam curve. Then the string is unwound from the curve and is kept stretched. The other end point describes the involute. The portion of the string which is unwound from the curve has zero curvature and its shape is close to the portion of the beam that is close to the tool-end as described earlier; the portion which is still wound along the curve remains the same curvature. From the earlier discussion, it is known that the latter portion almost has the same shape as the portion of the beam which is close to the free-end. ♦

Now we are in the position to describe the insertion phase of the tight tolerance assembly. First, start the insertion phase as in the loose clearance case. If the tool feels a large resistance and the beam cannot be inserted into the hole, the tool should go back to its original point. The tool is then moved by a small distance along the curve $\beta(t_0)$. The insertion is then tried again. If the resistance can be overcome, the insertion continuous. Otherwise, another adjustment is needed. The adjustment continues until the insertion become possible. During the insertion process, the tool should follow the beam curve for the same reason as discussed in the previous

section. Since the beam shape is very close to the curve of the string as just described, the trajectory of the tool is a straight line motion followed by a curved motion. The straight line motion is defined by $\alpha(t_0)$-$\beta(t_0)$ and the curved motion should follow the free beam curve after the tool touches the point $\alpha(t_0)$.

To feel the resistance force, one may install a force sensor at the end-effector. Alternatively, one may use a vision sensor to observe the shape of the beam curve. If a curve similar to the one as shown in Fig. 6b appears, the insertion encounters a large resistance and the adjustment becomes necessary. Otherwise, the tool can continue its motion following the beam curve.

6. EXPERIMENTAL RESULTS

To verify the assembly mechanisms as proposed in the previous sections, experiments were conducted in the Advanced Manufacturing Laboratory of the Ohio State University. The end-effector of a PUMA robot held a aluminum beam and inserted it into a hole. The beam was 0.44 m long, 0.024 m wide and 0.0005 m thick. The hole had the same size as the beam, but its thickness was adjustable such that the clearance between the hole and the size could be altered.

In order to conduct the experiment, we must first be able to describe the deflection of the beam. To do so, the term $\frac{\omega}{EI}$ contained in (6), (7) and (8) need to be identified. A vision system was used for this purpose. The details of the vision method are reported in [11] and will not be further discussed in this paper. Here only a brief description is provided.

Taking the first five terms of equation (6), the relationship between θ and θ_0 at $s = L$ can be obtained as follows:

$$\theta = \theta_0 + \frac{1}{6}\left(\frac{\omega}{EI}\right)\cos\theta_0 L^3 - \frac{1}{180}\left(\frac{\omega}{EI}\right)^2 \sin\theta_0 \cos\theta_0 L^6$$

$$+\frac{1}{8640}\left(\frac{\omega}{EI}\right)^3(\cos\theta_0)^3 L^9 - \frac{1}{12960}\left(\frac{\omega}{EI}\right)^3(\sin\theta_0)^2\cos\theta_0 L^9. \quad (29)$$

From (29), it can be seen that when $\frac{\omega}{EI}L^3$ is small (it is true for most flexible beams), five terms are enough to give a very close approximation. Otherwise more terms need to be included. Let the end-effector of the PUMA pick up the beam and hold it at a horizontal direction such that $\theta = 0$ degree. Using vision system, one can identify the deflection angle θ_0 at the free-end ([11]). With θ, θ_0 and L known, one can use (29) to calculate the term $\frac{\omega}{EI}$. Once the latter term is calculated, one can determine the required position and orientation of the tool in the approaching phase as well as the shape of the beam curve using (6), (7) and (8) (taking the first five terms, for example), or (9), (10) and (11).

The vision system can also be used to identify the shape of the beam curve by identifying a number of discrete points on the beam once the the free-end contacts the hole. The motion of the tool can then be approximated by piece-wise linear motions between the discrete points. In this way, lengthy computation for identifying the beam curve is not required.

The setup of the experiment is shown in Fig. 8. The part which has the hole is held static (the right side of the figure). The hole axis is thirty degrees from the horizontal direction, i.e., $\theta_0 = 30^o$. Based on the hole orientation, the tool position and orientation are calculated to be x=0.435m, y = 0.002m and θ= 0 degree. The shape of the beam curve in our experiment is identified by the vision system. Two assembly tasks were executed, one for the loose clearance and the other for the tight clearance. Fig. 9 shows the sequence of the loose clearance case, where a is the initial insertion phase, b is the insertion phase, and c is the end of the insertion phase (note that Fig. 8 also shows the approaching phase). In the insertion phase, the tool followed the beam curve that was identified by the vision system, and a successful assembly was achieved.

In the tight clearance experiment, we first let the tool follow the beam curve without any adjustment, and found that the beam could not go into the hole. As the tool moved towards the hole, the beam was badly deflected (Fig. 10a). Note that the vision system was also used to identify the abnormal deflection as mentioned earlier. By using the adjustment mechanism as discussed in the previous section, the tool came back to the original point, and was then adjusted following the involute by fifteen degrees. After that, the tool follow the new beam curve and the assembly was successfully completed (Fig. 10b).

7. CONCLUSIONS

Mechanisms for assembly of deformable parts have been presented in this paper. A flexible beam being inserted into a rigid hole was chosen as the target of study. The deflection behavior of the beam was first studied. Then conditions of successful assembly for rigid parts were reviewed. It was argued that conditions for rigid parts were applicable to deformable beams since the surface of the beam that contacted with the hole was still rigid. Based on the assembly conditions, tool trajectories were identified as the key issue for a successful assembly. Assembly mechanisms were proposed for both the loose and tight clearance cases. In the loose clearance case, the tool trajectory should follow the free beam curve to complete the insertion. In the tight clearance case, the trajectory should be adjusted according to the tightness of the clearance, and the adjustment should follow the involute of the free beam curve. Experiments were conducted for both loose and tight clearance cases. Successful results proved that the mechanism proposed in this paper are valid for mating flexible beams with rigid holes.

REFERENCES

1. Digital Equipment Corporation, "Cost analysis of the PWB assembly process," Private Communication.

2. M. Petry and W. Bick, "Automatic insertion of insulating mats on car assembly line," Assembly Automation, 8(4), 183- 185, 1988.

3. G. G. Hastings, W. J. Book, "Verification of a linear dynamic model for flexible robotic manipulator," in Proc. 1986 IEEE Int. Conf. on Robotics and Automation, San Francisco, CA, April 7-10, 1986, pp. 1024-1029.

4. S. Yurkovich, F.E. Pacheco and A. P. Tzes, "On-line frequency domain information for control of a flexible-link robot with varying payload, " in Proc. 1989 IEEE Int. Conf. on Robotics and Automation, Scottsdale, AZ, May 14-19, 1989, pp. 876-881.

5. S. B. Choi, B. S. Thompson and M. V. Gandhi, "Modeling and control of a ingle-link flexible manipulator featuring a graphite-kpoxy composite arm, " in Proc. 1990 IEEE Conf. on Robotics and Automation, Cincinnati, OH, May 13-18, 1990, pp. 1450 -1455.

6. S. Simunovic, "Force information in assembly process," in Proc. 5th Int. Symp. on Industrial Robots, Chicago, IL, Sept. 1975, pp. 415 - 431.

7. D.E. Whitney, "Quasi-static assembly of compliantly supported rigid parts," ASME, J. of Dynamics, Measurement, and Control, March, 1982, Vol. 104, pp. 65-77.

8. G. Buchanam, Mechanics of Materials, Holt Rinehart and Winston, Inc. New York, 1988.

9. F. V. Rhode, "Large deflections of cantilever beam with uniformly distributed load," Q. Appl. Math., pp. 337-338, Vol. 11, No. 3, 1953.

10. R. Frisch-Fay, Flexible Bars, Butterworth & Co. (Publishers) Limited, Washington, DC, 1962

11. C. Chen and Y.F. Zheng, "Deformation identification of one-dimensional objects by vision sensors," to appear.

12. Y.F. Zheng and F.R. Sias, "Two arms in assembly," in Proc. 1986 IEEE Int. Conf. on Robotics & Automation, San Francisco, CA, April 8-10, pp. 1230 - 1235.

13. R.S. Millman and G. D. Parker, Elements of Differential Geometry, Prentice-Hall Inc., Englewood Cliffs, NJ, 1977.

14. L. P. Eisenhart, An Introduction to Differential Geometry, Princeton University Press, Princeton, 1940.

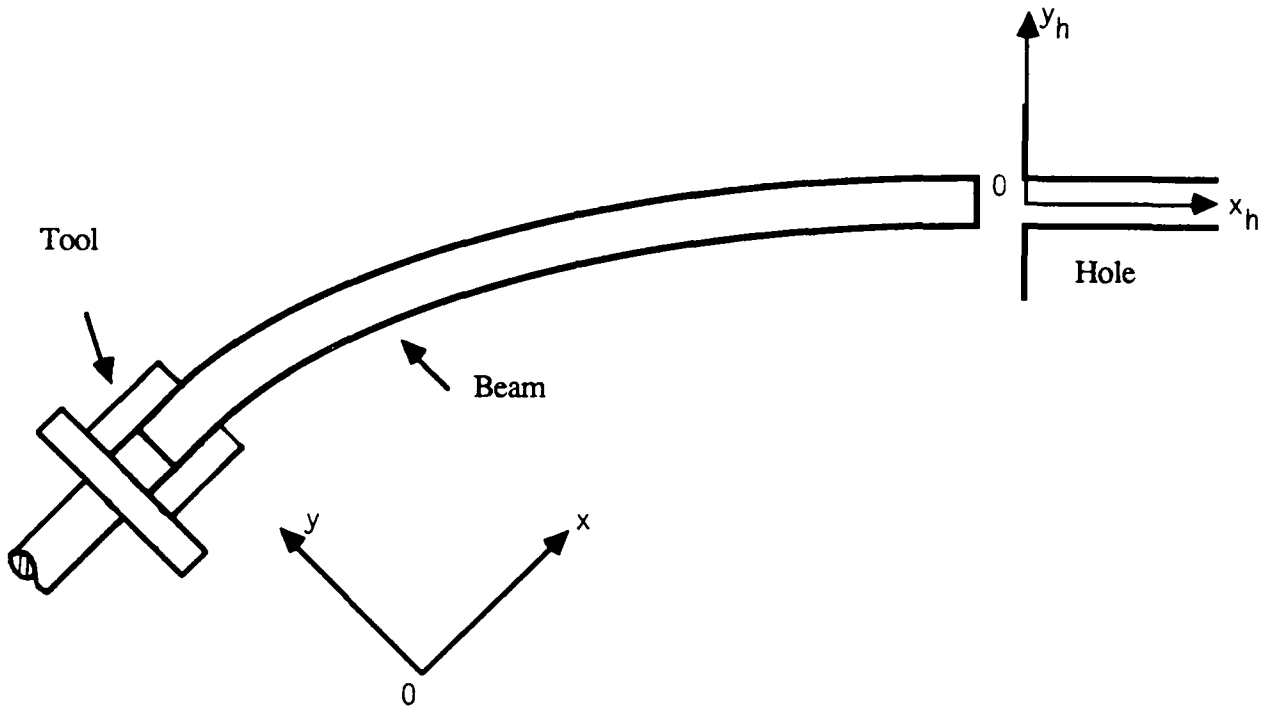

Fig. 1 A deflected beam is to be inserted into a hole

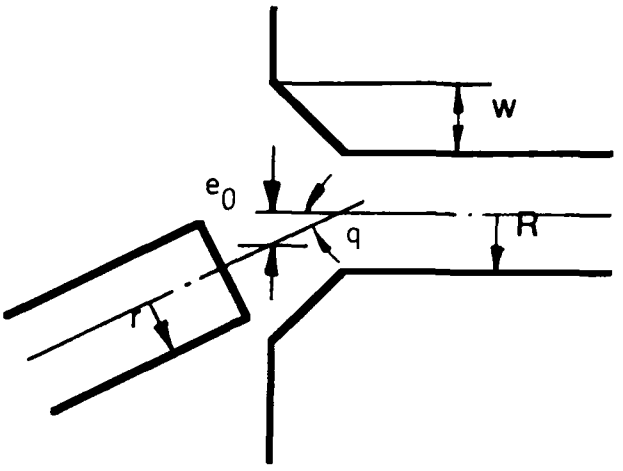

a. Geometric relations in peg insertion

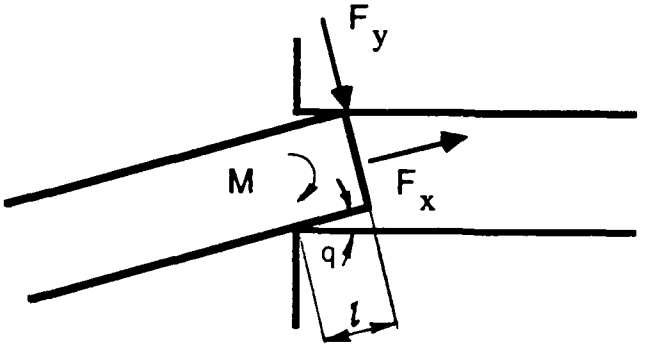

b. Reaction forces between the peg and the hole

Fig. 2 Geometry (a) and forces (b) in peg insertion

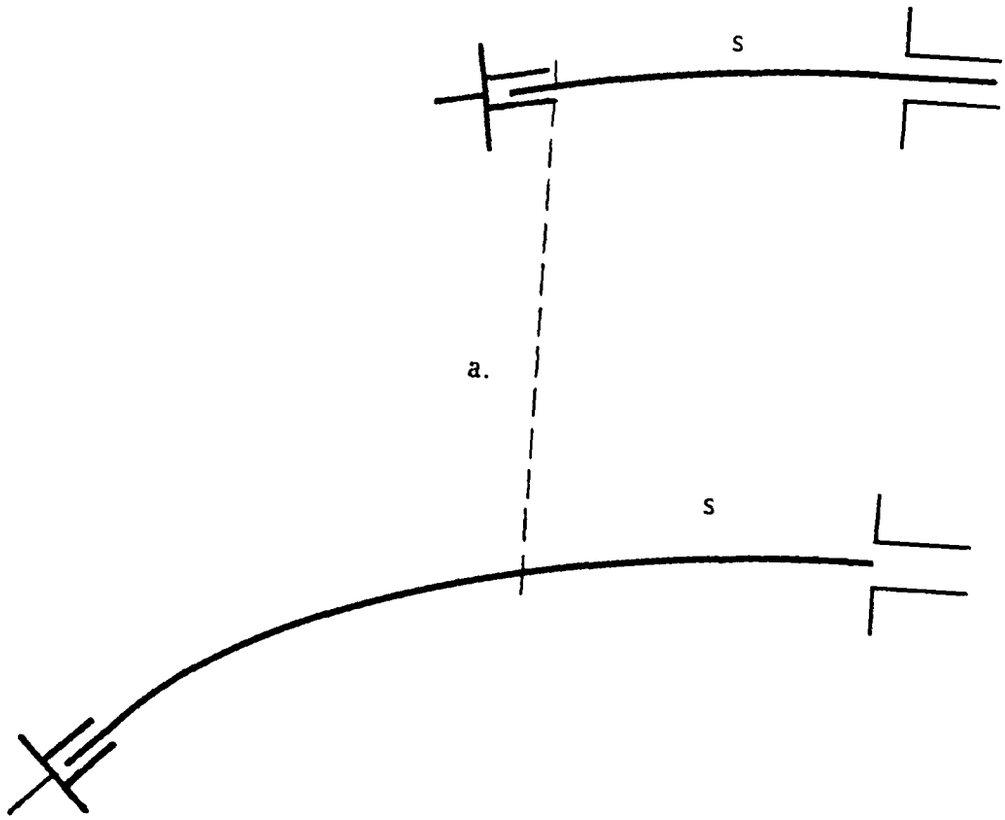

Fig. 3 The beam curve in (a) is the same as the portion in (b) which has the same length from the end of the beam (on the right of the dashed line).

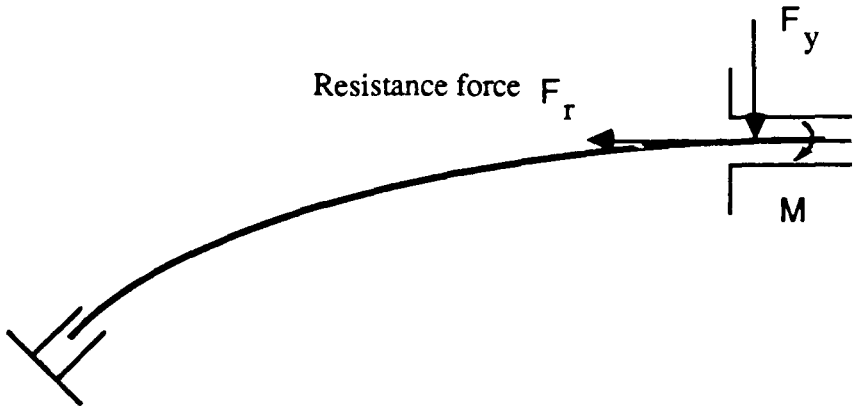

Fig. 4 In order to counterbalance the resistance force additional force and moment are necessary

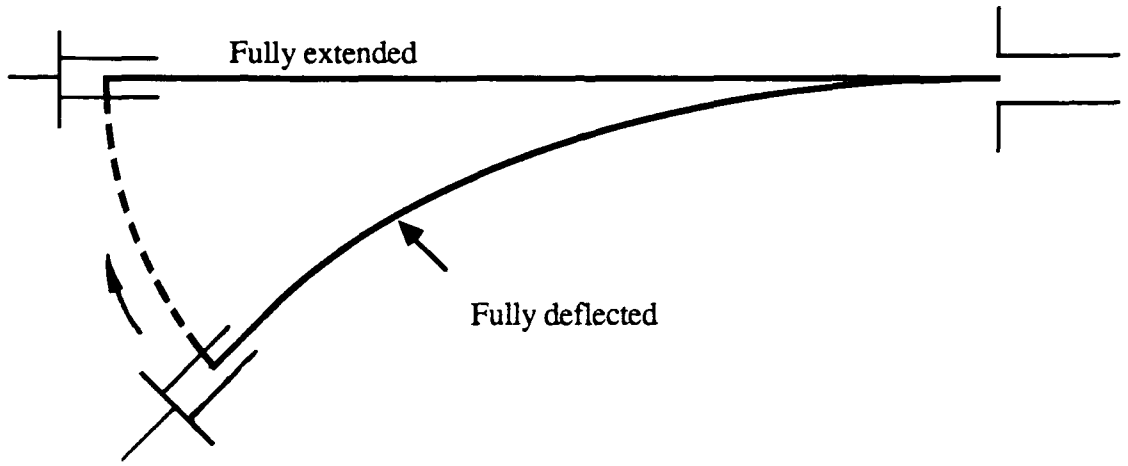

Fig. 5 The beam curves between fully extended and fully deflected

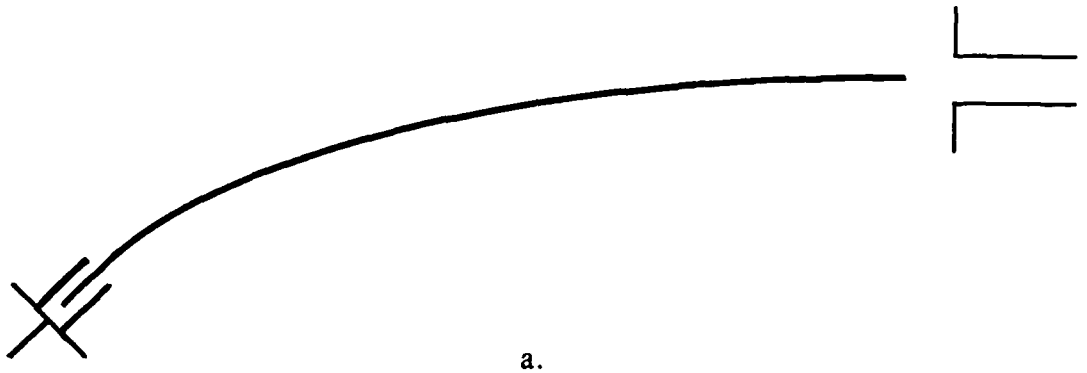

a.

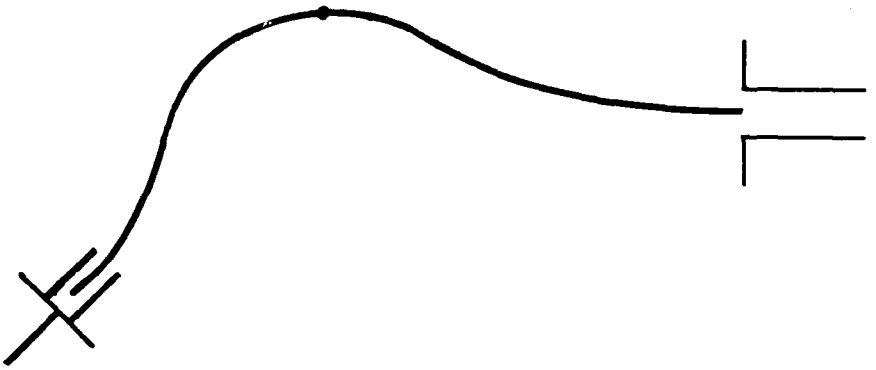

b.

Fig. 6 a. Tool is too far away from the hole, beam loses contact.
b. Tool is too close to the hole, beam is badly deflected.

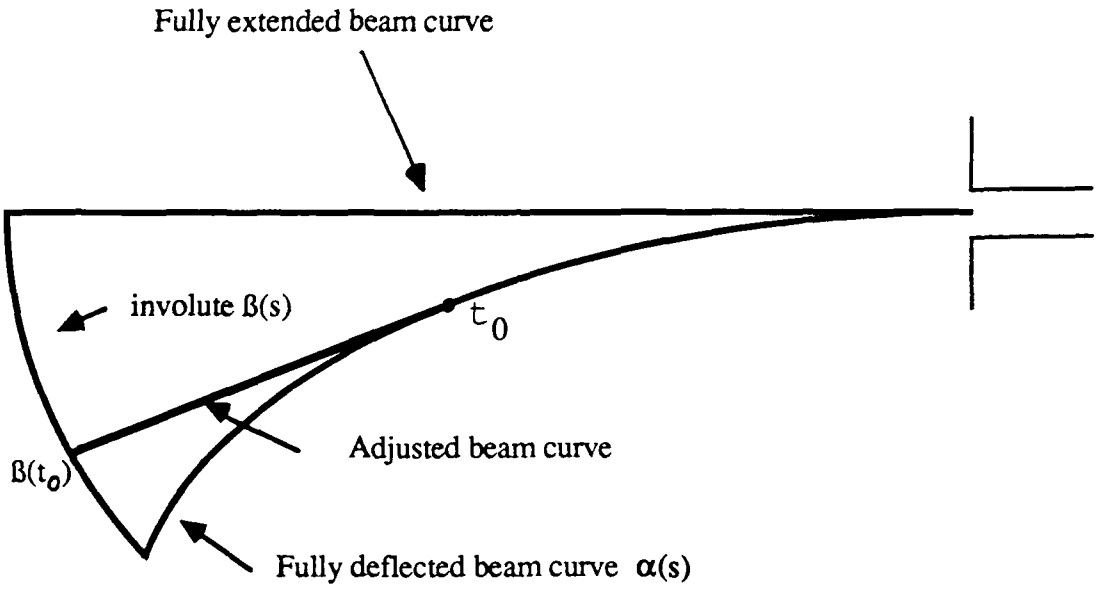

Fig. 7 The relation between the beam curve and its involute

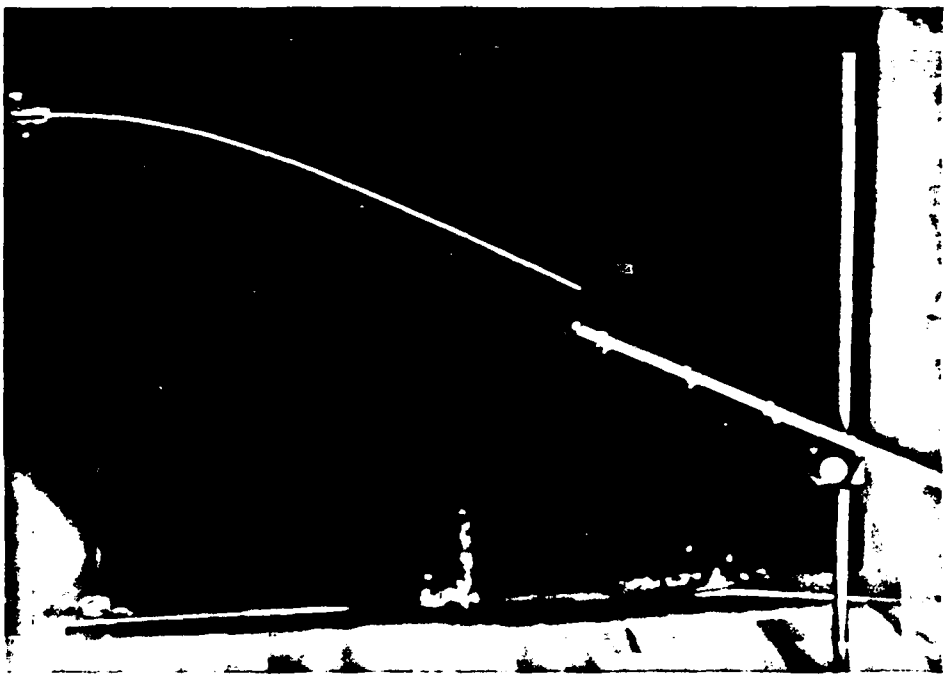

Fig. 8 The setup of the beam insertion experiment

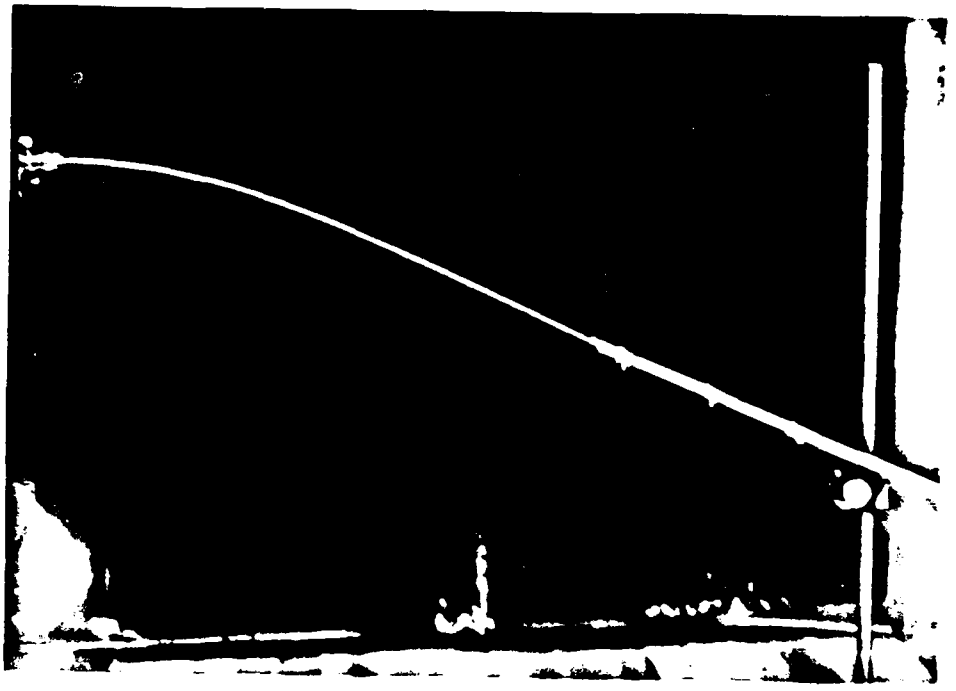

a. The initial insertion phase

Fig. 9 The sequence of the loose-clearance assembly (Cont'd)

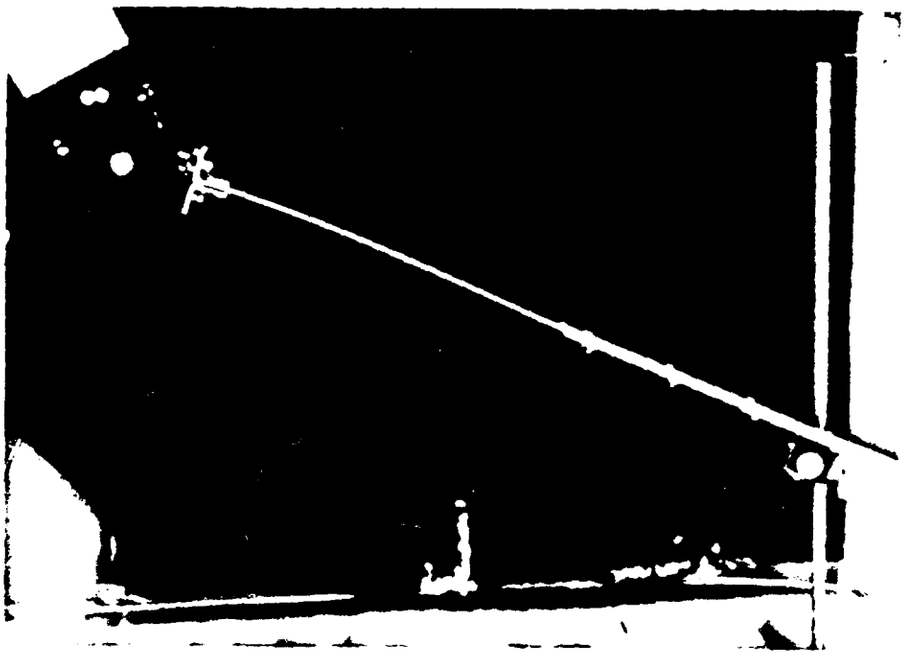

b. The insertion phase

Fig. 9 The sequence of the loose-clearance assembly (cont'd)

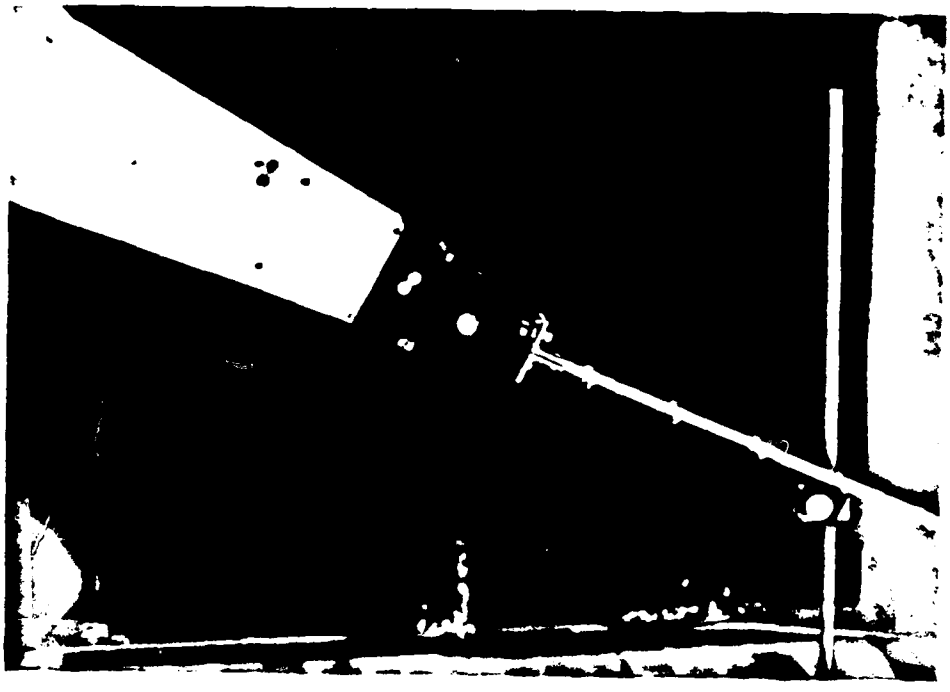

c. The end of the insertion phase

Fig. 9 The sequence of the loose-clearamce assembly

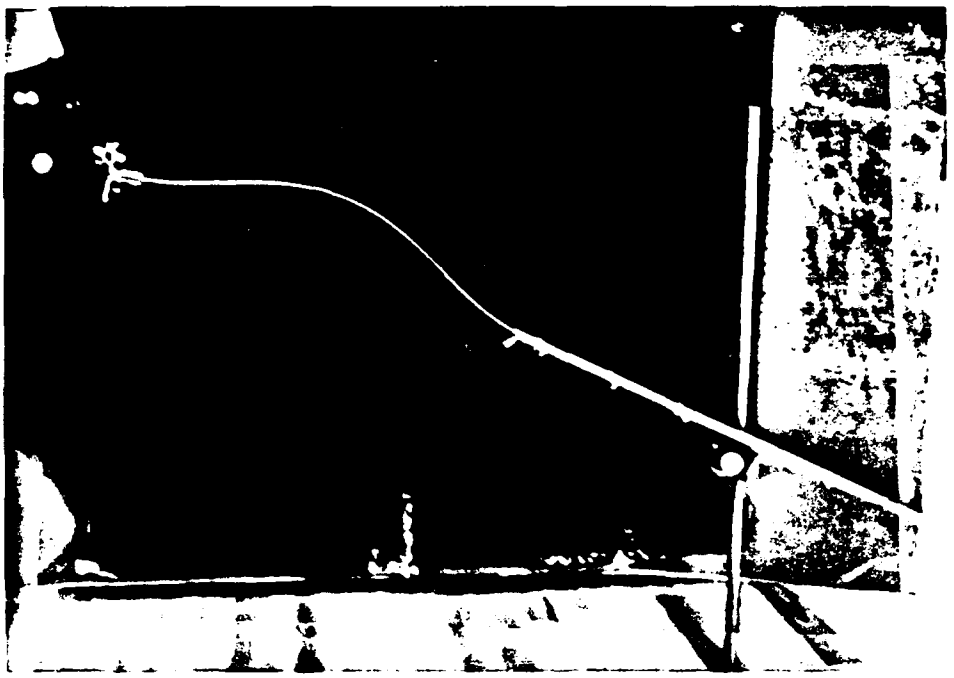

a. Without adjustment, the beam starts buckling

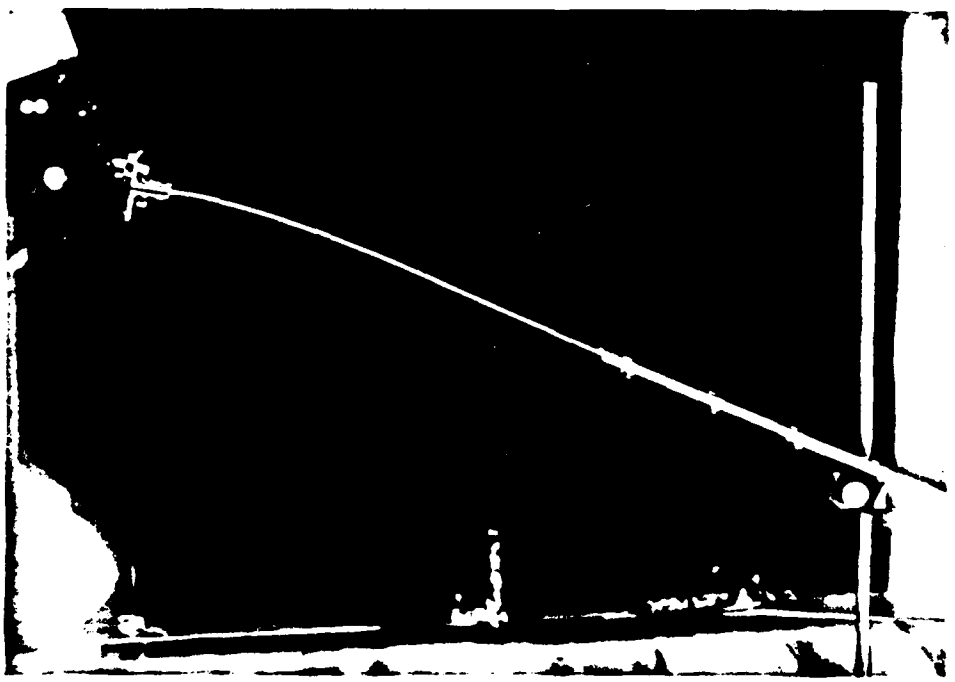

b. With adjustment, the beam is being inserted into the hole

Fig. 10 The experiment of the tight-clearance assembly

APPENDIX B

DEFORMATION IDENTIFICATION AND ESTIMATION OF ONE-DIMENSIONAL OBJECTS BY VISION SENSORS[1]

Chichyang Chen and Yuan F. Zheng

Department of Electrical Engineering
The Ohio State University
2015 Neil Avenue
Columbus, OH 43210

Abstract

Using vision sensors to study object deformation is introduced in this paper. The vision sensor is used to identify the deformation characteristic and estimate the deformation behavior of flexible beams. First, a nonlinear equation describing the deformation of the beam is given. Then, cubic spline functions are used to approximate the contour of the deformed beam after the beam is detected by the vision sensor. From the cubic spline approximation and using Maclaurin's series expansion, a procedure to determine the deformation characteristic is formulated. To estimate the deformation behavior, numerical differential method to solve the nonlinear equation is used. The error of this numerical method can be controlled with the aid of the vision sensor. Finally, experimental results are given to verify that the proposed methods are effective.

[1]Acknowledgment: This work is supported by the Office of Naval Research under grant N0014-90-J-1516

I. Introduction

In the areas of manufacturing automation and robotics, vision sensors have been widely used to recognize, locate, and describe objects in unstructured environment. In most cases, the objects are assumed to be rigid, which means that the objects will not change their size and shape during the process of assembling. In reality, deformable objects are often encountered in many situations. For example, in shipbuilding, aerospace and automobile industries, flexible plates are often used for assembling various vehicles. Even rigid objects become deformable when their size is large. When the objects are deformable, their size and shape will change during the process of assembling. As a result, it becomes difficult to locate the position and orientation of the objects. In fact, the deformable objects have already become a part of the unstructured environment.

In this paper, a new application of vision sensors is introduced. The vision sensor is used to identify the deformation characteristic of deformable objects. After the deformation characteristic is found, the deformation behavior of the objects can be estimated and the automatic handling and assembling of the objects can be accomplished. As an illustration of the new application of vision sensors, we first chose one-dimensional objects as our research target and will extend our study to two- and three-dimensional cases in the future. Without loss of generality, we also assume that the objects have only elastic deformation. However, we do not limit the size and the amount of the deformation of the objects.

For a one-dimensional deformable object, that is, a flexible beam, the deformation can be described by the following equation,

$$EI\frac{1}{\rho} = EI\frac{d\theta}{ds} = M(s), \tag{1}$$

where ρ is the radius of curvature, E is the stiffness of the material, I is the moment

of inertia of the cross-sectional area, s is the length of the beam, θ is the angle from the x-axis to the tangential vector at point s, and $M(s)$ is the deflecting moment exerting at point s of the beam. For convenience, θ is referred to as the **deflection angle** hereafter. Because $M(s)$ also depends on θ, equation (1) is difficult to solve. If we take the derivative on each side of equation (1), and assume the origin being at the free-end of the beam [1][2], equation (1) becomes

$$\frac{d^2\theta}{ds^2} = -\frac{w}{EI} s\cos\theta, \tag{2}$$

where w is the weight density of the beam. From equation (2), the deformation of the beam is completely determined by the term $\frac{w}{EI}$ and the length of the beam. For simplicity, the length of the beam is assumed to be known. The only unknown remained to be found is $\frac{w}{EI}$. Since $\frac{w}{EI}$ determines the deformation of the beam, it is referred to as the **deformation characteristic** of the beam.

Equation (2) is nonlinear and has no closed-form solution for θ. Although many numerical methods can provide approximate solution for θ, we must choose ones that are explicitly expressed in terms of s and $\frac{w}{EI}$ so that the observed θ's from the detection of the vision sensor can be utilized to determine $\frac{w}{EI}$. The numerical method we chose to determine $\frac{w}{EI}$ is Maclaurin's series expansion, since it expresses θ explicitly in terms of s and $\frac{w}{EI}$.

Although the method using Maclaurin's series expansion to solve equation (2) is efficient in identifying the $\frac{w}{EI}$, its error in approximating θ is not controllable when the length of the beam or $\frac{w}{EI}$ becomes large. So, in estimating the deformation behavior of the beam, another method which is more robust in controlling the error is introduced. This method, named as **numerical differentiation** method, approximates the second derivative in equation (2) by Lagrangian interpolation formula. The numerical differentiation method and the Maclaurin's series expansion are discussed in detail in the sequel.

For the purpose of identifying the deformation characteristic and manipulating the deformed beam, the contour of the deformed beam needs to be described by mathematical equations. Since equation (2) has no closed-form solution, it is impossible to find an exact equation to describe the contour of the deflected beam in terms of s. Approximation has to be made in expressing the curve of the beam after the vision sensor detects the edge points of the beam. The cubic spline functions are very suitable for approximating the contour of the deflected beam. They have two important properties. One is that their first and second derivatives are continuous and the other is that they approximately represent a physical spline with minimum internal strain energy which resembles the nature of a deformed beam [3].

Speed is an important issue when vision sensors are used in automation. Usually, vision processing is time-consuming because complicate vision algorithms have to work on a large amount of data. Fortunately, because the deflected beam can be approximated by cubic spline functions, only certain discrete edge points of the beam need to be detected by the vision sensor. To further increase the speed of the detection of the edge points of the beam, the illumination of the workplace is designed to make the brightness of the edge points on the beam much higher than the background. So, only simple one-dimensional edge detection algorithm has to be performed to detect the edge points of the beam.

To verify that the proposed methods in identifying and estimating the deformation of the beam is effective, an experiment was conducted. An aluminum beam held by the robot's gripper was tested. The experimental results show us that the methods are effective.

As an illustration of the new application of vision sensors, another experiment was also made. The vision sensor was used in guiding the robot's gripper in the process of inserting the flexible aluminum beam into a rigid straight hole. In order to insert the beam into the hole smoothly, the orientation of the contact point of

the beam with the inlet of the hole must be kept the same as that of the hole. The proposed methods in determining and estimating the deformation of a beam have successfully guided the gripper in the insertion process.

The organization of this paper is as follows. In Section II, vision detection of the beam is discussed. Section III gives the cubic spline approximation of the deflected contour of the beam. Section IV presents the identification of the deformation characteristic of the beam using the Maclaurin's series expansion, while Section V covers the estimation of the deformation behavior of the beam using the numerical differentiation method. The experimental results that verify the numerical methods are given in Section VI. The vision guided insertion of the aluminum beam into a rigid hole is described in Section VII. Section VIII concludes the paper.

II. Vision Detection of Deformed beam

Speed and accuracy are the two main considerations in choosing the method for beam detection. The most straightforward method is to detect all the edge points of the beam. This method has two drawbacks. One obvious drawback is that it is very time-consuming. The second is that, although it is accurate in determining the position of every edge point of the beam, the deflection angle θ at each point of the beam is difficult to be accurately determined since the edge points are discrete.

Instead of detecting all the edge points of the beam, the nature of the deformed beam should be examined to find out the most efficient and accurate method to detect and represent the beam. Since the first and second derivatives of the contour of the beam and the cubic spline functions are both continuous and the spline function has the property that its representation has the minimum strain energy, cubic spline functions are very suitable for approximating the contour of

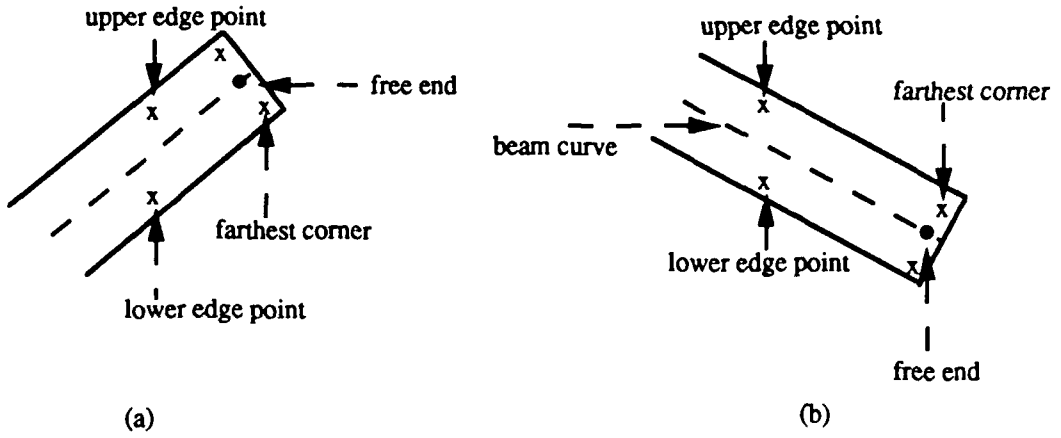

Figure 1: Image of deformed beams.

the deformed beam.

To apply the spline function to representing the contour of the deformed beam, certain edge points of the beam have to be detected. These points should include the end points of the beam and should be evenly distributed along the beam in order to have an accurate approximation for the curve of the beam. Since the amount of deformation of the beam is not known beforehand, we must first find out the position of the free end of the beam. After it is found and the fixed end of the beam is already known (which is the position of the gripper if the beam is manipulated by the gripper), the position of the other edge points between these two points can easily be detected by applying one-dimensional edge detection along the beam.

In this section, we first discuss how an edge point of the beam is detected and then describe how the free end can be found. In the discussions above and following, the geometric camera calibration is assumed to be done. The position of a point in space can be referred to a pixel in the image plane and vice versa.

A. Edge Point Detection

As shown in Fig. 1, the image of the deformed beam is a curved rectangular which is two-dimensional. The desired contour that can best represent the

deformation of the beam is the center line of the rectangular. This center line will be referred to as the **"beam curve"** and the points of the beam curve that are used in spline approximation is referred to as the **"knots"** of the beam hereafter.

The illumination of the workplace is so designed that the brightness of the beam is much higher than that of the background. Consequently, the edge points of the beam can be detected by using only one-dimensional difference and thresholding operations. The position of the knots is then at the middle of the upper and lower edge points of the beam.

B. Binary Search for the Free End

In searching for the free end of the beam, we assume that the length of the beam is already known and the background of the workplace is set up to be dark and uniform. The method for searching the free end can thus be described as follows.

Beginning from the midway of the beam, one-dimensional edge detection is applied. If an upper edge point and a lower edge point are found, then move forward one quarter length of the beam; otherwise, move backward one quarter length of the beam. Repeat this searching process with each movement being half the distance of its previous step until the distance of the movement is less than one pixel length. The edge point detected from the last edge detection is thus the farthest corner of the curved rectangular as shown in Fig. 1(a) and 1(b). The other corner of the rectangular can easily be detected. The free end is then the midpoint of these two corner points.

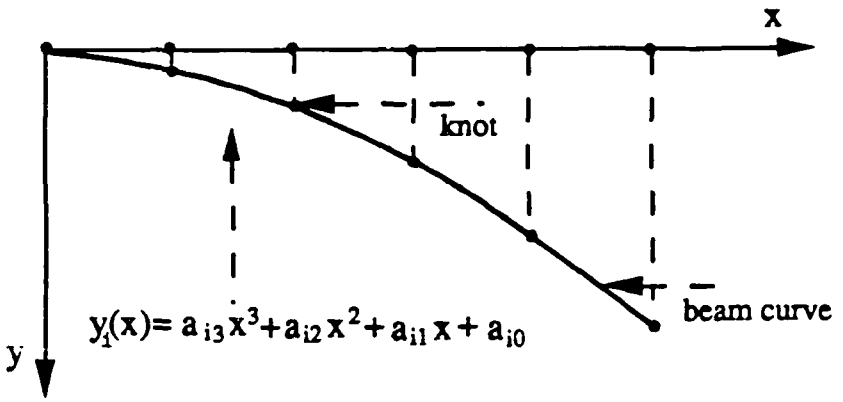

Figure 2: Beam curve and the knots.

III. Spline Approximation of the Beam Curve

Once the location of the free end and the other knots of the beam curve have been detected, each segment of the curve that is bounded by the knots can be approximated by a cubic polynomial. If there are $n+1$ knots, n cubic polynomials are required. As shown in Fig. 2, we assume that the beam curve is in the x-y plane, and the i-th segment of the beam curve is represented by

$$y_i(x) = a_{i3}x^3 + a_{i2}x^2 + a_{i1}x + a_{i0}. \tag{3}$$

Each cubic polynomial has four unknown coefficients. Thus, totally $4n$ unknowns have to be determined in order to approximate the whole beam curve.

These $4n$ unknowns can be solved by $4n$ conditions. The position of the $n+1$ knots and the continuity property of the spline functions gives $4n-2$ conditions explicitly, which are outlined as follows.

1. The position of $n+1$ knots gives $n+1$ conditions.

2. Continuity of y_i at the knots gives $n-1$ conditions.

3. Continuity of the first derivative of y_i at the knots gives $n-1$ conditions.

4. Continuity of the second derivative of y_i at the knots gives $n-1$ conditions.

Two more conditions can be found from the boundary conditions at the two end points of the beam curve.

At the fixed end of the beam, the first derivative of y_1 is equal to the tangent of the angle of the gripper which is already known. That is, $y_1'(0) = \tan(\theta_{gp})$, where θ_{gp} is the angle of the gripper.

The other boundary condition is at the free end of the beam. Because the moment exerted on the free end is zero, we can see from the following equation

$$M(x) = EI\frac{1}{\rho} = EI\frac{\frac{d^2y}{dx^2}}{[1+(\frac{dy}{dx})^2]^{\frac{3}{2}}}. \tag{4}$$

that the second derivative of y_n at the free end is zero. That is, $y_n''(x_n) = 0$, where x_n is the x-coordinate of the free end.

IV. Identification of the Deformation Characteristic

The difficulty in identifying the deformation characteristic, $\frac{w}{EI}$, of the beam results from the nonlinearity of equation (2) which has no closed form solution for θ. Explicit expression of θ in terms of s and $\frac{w}{EI}$ must be given so that $\frac{w}{EI}$ can be derived by using the cubic spline representation of the detected beam curve. In the following, the Maclaurin's series approximation for θ is given first. Then a sufficient condition for the series to converge and the error of the approximation are analyzed. And a procedure to determine the deformation characteristic $\frac{w}{EI}$, by taking the convergence condition of the series into consideration, is described.

The Maclaurin's series expansion of $\theta(s)$ is

$$\theta(s) = \theta(0) + \frac{1}{1!}\theta'(0)s + \frac{1}{2!}\theta''(0)s^2 + ... + \frac{1}{(n-1)!}\theta^{(n-1)}(0)s^{n-1} + R_n(s), \tag{5}$$

where

$$R_n(s) = \frac{1}{n!}\theta^{(r)}(\xi)s^n$$

is the remainder of the expansion and $\xi \in [0, s]$. From equation (2) and the boundary conditions $\theta(0) = \theta_0, \theta'(0) = 0$, and $\theta''(0) = 0$, we have

$$\begin{cases} \theta^{(3)}(0) &= -\frac{w}{EI}\cos(\theta_0) \\ \theta^{(4)}(0) &= \theta^{(5)}(0) = 0 \\ \theta^{(6)}(0) &= -4(\frac{w}{EI})^2 \sin(\theta_0)\cos(\theta_0) \\ \theta^{(7)}(0) &= \theta^{(8)}(0) = 0 \\ \theta^{(9)}(0) &= 42(\frac{w}{EI})^3\cos^3(\theta_0) - 28(\frac{w}{EI})^3\sin^2(\theta_0)\cos(\theta_0). \end{cases} \tag{6}$$

Thus,

$$\begin{aligned} \theta(s) = \quad & \theta_0 - \tfrac{1}{6}\cos(\theta_0)(\tfrac{w}{EI})s^3 - \tfrac{1}{180}\sin(\theta_0)(\tfrac{w}{EI})^2\cos(\theta_0)s^6 + \tfrac{1}{8640}\cos^3(\theta_0)(\tfrac{w}{EI})^3 s^9 \\ & -\tfrac{1}{12960}\sin^2(\theta_0)\cos(\theta_0)(\tfrac{w}{EI})^3 s^9 + \tfrac{1}{10!}\theta^{(10)}(0)s^{10} + \ldots\ldots + R_n(s). \end{aligned} \tag{7}$$

Since there is no exact explicit expression for $\theta(s)$, neither for $\theta^{(n)}(s)$, the necessary condition for the series (5) to converge is unknown. However, from equation (7), each term (except θ_0) contains a factor of $\frac{w}{EI}s^3$. So, a sufficient condition for (5) to converge can be obtained. If the value of s can satisfy $\frac{w}{EI}s^3 \leq 1$, then (5) can converge. In addition, the maximum error in approximating θ can be determined. For example, if we take $n = 9$ in (7), then

$$\theta(s) \approx \theta_0 - \frac{1}{6}(\frac{w}{EI})\cos(\theta_0)s^3 - \frac{1}{180}(\frac{w}{EI})^2\sin(\theta_0)\cos(\theta_0)s^6, \tag{8}$$

and the error in approximating $\theta(s)$ is

$$R_9 = [\frac{1}{8640}\cos^3(\theta(\xi)) - \frac{1}{12960}\sin^2(\theta(\xi))\cos(\theta(\xi))](\frac{w}{EI})^3 s^9$$

which is less than $\frac{1}{8640} = 1.16 \times 10^{-4}$.

If the length of the beam is l, then we can categorize the beam as either large deflection beam if $\frac{w}{EI}l^3 > 1$ or small deflection beam if $\frac{w}{EI}l^3 \leq 1$. To decide the beam as either small or large deflection beam, the deflection angle, θ_l at $s = l$ is compared to an angle

$$\theta_a \equiv \theta_0 - \frac{1}{6}\cos(\theta_0) - \frac{1}{180}\sin(\theta_0)\cos(\theta_0) + \frac{1}{8640}\cos^3(\theta_0) - \frac{1}{12960}\sin^2(\theta_0)\cos(\theta_0).$$

If $\theta_l \geq \theta_a$, the beam is a small deflection beam. Otherwise, it is a large deflection beam.

The procedure for determining the deformation characteristic $\frac{w}{EI}$ can then be stated as follows.

1. If the beam is a small deflection beam, that is, $\theta_l \geq \theta_a$, then $\frac{w}{EI}$ can be derived very accurately from the following equation

$$\begin{aligned}\theta_l = \quad & \theta_0 - \tfrac{1}{6}\cos(\theta_0)(\tfrac{w}{EI})l^3 - \tfrac{1}{180}\sin(\theta_0)\cos(\theta_0)(\tfrac{w}{EI})^2 l^6 + \\ & \tfrac{1}{8640}\cos^3(\theta_0)(\tfrac{w}{EI})^3 l^9 - \tfrac{1}{12960}\sin^2(\theta_0)\cos(\theta_0)(\tfrac{w}{EI})^3 l^9,\end{aligned} \tag{9}$$

   where θ_l is exactly the gripper's angle and θ_0 is the deflection angle at the free end which can be derived from the spline approximation of the beam curve,

$$\theta_0 = \tan^{-1}(3a_{n3}x_n^2 + 2a_{n2}x_n + a_{n1}),$$

   with x_n the x-coordinate of the free end of the beam.

2. If $\theta_l < \theta_a$, then $\frac{w}{EI}l^3 > 1$, which means that equation (5) might not converge. Since we already have the spline description of the beam curve, we can find out a point $\mathrm{A}(x_a, y_a)$ of the beam curve whose deflection angle is equal to θ_a.

3. Calculate the length a from the free end to the point A by the following approximation

$$a = \sum_{i=1}^{m} \Delta x_i \sec(\theta_i),$$

where $\theta_i = \tan^{-1}(3a_3x_i^2 + 2a_2x_i + a_1)$ is the deflection angle at the discrete point x_i, $\Delta x_i = (x_n - x_a)/m$, and m can be chosen as large as possible.

4. Finally, $\frac{w}{EI} = a^{-3}$ since at point A, $\theta(a) = \theta_a$.

V. Deformation Behavior Estimation

For the purpose of automatic manipulation of the deformable objects, the deformation behavior of the objects must be estimated before manipulation. For the case of one-dimensional objects, this means that the position and orientation of the gripper needed to reach the desired pose of the object should be estimated. In particular, given the desired position and orientation of the free end of the beam, the required position and orientation of the manipulator is of more interest to us if the fixed end of the beam is held by the manipulator. Instrumental in answering this question is the choice of the numerical method to solve equation (2) and how the error is controlled. In the following, the choice of the numerical method is discussed first. The control of the numerical error with the aid of the vision sensor is described next.

A. Choice of numerical method

Under the condition $\frac{w}{EI}l^3 \leq 1$, the Maclaurin's series expansion is a very effective method to solve equation (2). The series approximating $\theta(s)$ converges and the error is under control. Given the desired deflection angle θ_0 of the free end of the beam, the angle θ_l of the gripper should be

$$\theta_l = \theta_0 - \frac{1}{6}\cos(\theta_0)(\frac{w}{EI})l^3 - \frac{1}{180}\sin(\theta_0)\cos(\theta_0)(\frac{w}{EI})^2 l^6 + \frac{1}{8640}\cos^3(\theta_0)(\frac{w}{EI})^3 l^9 - \frac{1}{12960}\sin^2(\theta_0)\cos(\theta_0)(\frac{w}{EI})^3 l^9, \quad (10)$$

and the maximum error of θ_l is much less than 1.16×10^{-4} if the n in equation (5) is chosen to be twelve. However, when $\frac{w}{EI}l^3 > 1$, not only the error in approximating $\theta(s)$ could become very large if the n is fixed, but also the convergence of the series is not assured. Since the factor $\frac{w}{EI}$ is not known beforehand, the Maclaurin's series method is not robust in estimating the deformation behavior of the beam.

Once the deformation characteristic $\frac{w}{EI}$ of the beam has been identified, numerous methods can be used to solve equation (2). In the following, a method that is derived from [4] and can be applied to all values of $\frac{w}{EI}l^3$ is described.

Firstly, the length l of the beam curve is divided equally into n small segments, each with length h. Then, replacing the second derivative in the left side of equation (2) with the divided difference approximation derived from the Lagrangian interpolation formula, equation (2) becomes

$$\theta_{i+2} - 2\theta_{i+1} + \theta_i = h^2(\frac{-w}{EI})s_{i+1}\cos(\theta_{i+1}), \quad (11)$$

where θ_i denotes $\theta(s_i)$ and $s_i = ih$ for $i = 0, 1, 2, ..., n$, and the local truncation error is

$$\frac{h^4}{12}\theta^{(4)}(\xi), \text{ with } \xi \in [s_i, s_{i+2}]. \quad (12)$$

Equation (11) is an explicit method to compute $\theta(s_n)$. However, to start the computation, we need θ_0 and θ_1. θ_0 is already known. θ_1 can be obtained from the Lagrangian quadratic interpolation of $\theta'(s_0)$ which is

$$\theta'(s_0) = (2h)^{-1}(-\theta_2 + 4\theta_1 - 3\theta_0), \quad (13)$$

and the truncation error of the interpolation is

$$\frac{2h^2}{3!}\theta^{(3)}(\eta), \eta \in [s_0, s_2]. \tag{14}$$

Since $\theta'(s_0) = \theta'(0) = 0$ and $\theta(s_0) = \theta_0$, it turns out that

$$\theta_1 = \frac{1}{4}\theta_2 + \frac{3}{4}\theta_0. \tag{15}$$

With $i = 0$ and substituting θ_1 with equation (15), equation (11) becomes

$$\theta_2 = \theta_0 - 2h^3(\frac{w}{EI})\cos(\frac{1}{4}\theta_2 + \frac{3}{4}\theta_0). \tag{16}$$

θ_2 can be derived from equation (16) by iterative method. After θ_2 is known, θ_1 can also be obtained. Computation of equation (11) can proceed and θ_i, for $i = 3, 4, ..., n$, can be computed.

After θ_i's are obtained, the coordinate (x_i, y_i) of each discrete point of the beam can be calculated by

$$x_i = \sum_{j=0}^{i} h\cos(\theta_j), \text{ and } y_i = \sum_{j=0}^{i} h\sin(\theta_j).$$

B. Vision Aided Error Control

Three kinds of error occur in the computation of θ_i's in equation (11). The first is the truncation error which results from the Lagrangian interpolation of the derivatives. As shown in equations (12) and (14), this error is proportional to the power of h. The second kind of error is from the round-off error occurs at some decimal place. On the contrary, the round-off error is inversely proportional to the power of h, which is shown in this section. The last kind of error is from the inaccuracy of $\frac{w}{EI}$ which in turn results from the error of the vision sensor and the spline approximation of the beam curve. From equation (11), the error caused by the inaccuracy of $\frac{w}{EI}$ will be accumulated as the computation of θ_i's proceeds and is a nonlinear function of $\frac{w}{EI}$ and h. The choice of n thus affect heavily the accuracy of the numerical method since $h = l/n$.

Because the error caused by the inaccuracy of $\frac{w}{EI}$ is a nonlinear function of n (or h), there is no explicit method to determine the optimal n which will cause minimum error in the computation of θ_i's. However, adequate value of n which will make the error be within some range can be determined empirically with the aid of the vision sensor. This value of n can be derived in two steps. First, we determine a value of n, denoted by n' that will cause minimum error from local truncation and round-off by assuming that the value of $\frac{w}{EI}$ is accurate. Since the truncation error is proportional to the power of h and the round-off error is inversely proportional to the power of h, n' can be determined from equalizing the maximum truncation error and the maximum round-off error. Secondly, compute θ_l from (11) using n' and with θ_0 observed from the vision sensor. Then compare the computed θ_l with gripper's angle θ_{gp}. If the difference between these two values is smaller than the error of the vision sensor, the value of n' is the one required. Otherwise, adjust the value of n' until the difference is smaller than the error of the vision sensor. In the following, derivation of the value of n' in the first step is described.

The truncation error in the Lagrangian interpolation for $\theta'(s_0)$ is, from equation (14),

$$\frac{2h^2}{3!}\theta^{(3)}(\eta), \eta \in [s_0, s_2].$$

Since $|\theta^{(3)}(\eta)| \leq \frac{w}{EI}$, the maximum truncation error in this case is $\frac{2h^2}{3!}\frac{w}{EI}$. According to [5], the round-off error at point s_m, for $m = 0, 1, 2$ in the quadratic Lagrangian interpolation for $\theta'(s_0)$ is

$$R_1(m) = h^{-1}\sum_{j=0}^{2}\left|\frac{d}{dm}\sum_{i=0, i\neq j}^{2}\frac{(m-i)}{(j-i)}\right|\epsilon, \tag{17}$$

where ϵ is the round-off value at some decimal place. For example, in PUMA's VAL-II programming language, ϵ is equal to 5×10^{-6}. The value of h that equalizes the maximum truncation error and the maximum round-off error can be derived

from the following equation,

$$R_1(1) = \frac{2h^2}{3!}\frac{w}{EI}.$$

Because $R_1(1) = h^{-1}\epsilon$, the value of h is

$$(\frac{3\epsilon}{(\frac{w}{EI})})^{\frac{1}{3}}, \tag{18}$$

where the value $\frac{w}{EI}$ is obtained from vision's identification. So,

$$n' = \frac{l(\frac{w}{EI})^{1/3}}{(3\epsilon)^{1/3}}$$

Another value of h can also be derived from the truncation and round-off errors of the Lagrangian interpolation for $\theta''(s)$ with the same argument as discussed above. However, the value of h thus derived is several order less than that in (18). We conclude that the choice of h is from (18) and the dominant truncation and round-off errors are from (12) and (14).

VI. Experimental Results

An experiment was conducted to verify that the proposed methods for the vision identification and estimation of deformation of the beam is effective. An aluminum beam with length = $443mm$, width = $24mm$ and thickness = $0.5mm$ was tested. The beam was held by the gripper of a PUMA 560's arm. The vision sensor is Unimation's UniVision system which can allow the VAL-II controller access the grey level of an array of pixels of the image frame. The program in this experiment was written in VAL-II programming language.

Two kinds of tests were conducted on the beam. One is the identification of the deformation characteristic of the beam using the method described in Section IV. The orientation of the gripper holding the beam in this test is horizontal.

After the deformation characteristic of the beam is identified, the test of the numerical methods for estimating the deformation behavior was made. The numerical methods include both the Maclaurin's series expansion and the numerical differentiation method. Several cases of the desired angles of the free end were tested which includes $20°, 30°, 40°$, and $50°$. The results for these tests are outlined below. The notations in the following tables follow those in Section IV and V.

The results of the test for the identification of the deformation characteristic $\frac{w}{EI}$ are

θ_l	θ_0	a	$(\frac{w}{EI})_1$	$(\frac{w}{EI})_2$	$(\frac{w}{EI})_2 l^3$
$0°$	$27.36°$	$312mm$	$35.65m^{-3}$	$32.89m^{-3}$	2.856

where $(\frac{w}{EI})_1$ is derived from equation (9) and $(\frac{w}{EI})_2$ is derived from step (4) in the procedure discussed in Section IV.

The results of the test for the deformation estimation using Maclaurin's series method (equation (10) with $\frac{w}{EI} = 32.89$) are

Desired θ_0	Calculated θ_l	Observed θ_0
$20°$	$-6.38°$	$22.07°$
$30°$	$5.30°$	$31.00°$
$40°$	$17.84°$	$41.50°$
$50°$	$31.17°$	$49.52°$

The results of the test for the deformation estimation using the numerical differentiation method described in Section V with $\frac{w}{EI} = 32.89$ and $n = 230$ are

Desired θ_0	Calculated θ_l	Observed θ_0
20°	−7.92°	20.07°
30°	3.16°	30.41°
40°	17.24°	39.54°
50°	30.90°	49.87°

The results of the numerical differentiation method are better than those of the Maclaurin's series method, especially in the cases of smaller desired θ_0. The reason is when θ_0 is small, the degree of deformation of the beam is more severe.

VII. Vision Guided Automatic Assembly of Deformable Beam

Another experiment was also conducted to illustrate the usage of the proposed methods for the identification and estimation of the deformation of objects. The goal of the experiment is to insert the flexible aluminum beam into a rigid straight hole. Since the beam is flexible, strategies for the insertion of the beam into the hole is different from inserting a rigid beam. Detailed description about the strategies for the insertion of the flexible beam into the hole can be found in another paper [6].

The functions of the vision sensor in the process of insertion of the beam have three folds. The first is to identify the deformation characteristic of the beam and estimate the required angle of the manipulator so that the orientation of the free end of the beam is aligned with the hole before the insertion proceeds. The second function of the vision sensor is to determine the spline approximation of the beam curve after the free end of the beam has contacted the hole with their orientations aligned. It is claimed in [6] that the optimal trajectory of the manipulator for the insertion is the beam curve. The third function of the vision sensor is to detect any buckling of the beam during the process of the insertion. The buckling of the

beam is caused by the large fiction between the beam and the inside surface of the hole. The solution to the buckling is to adjust the court of the gripper following the involute of the free beam curve[6].

Two cases of insertion were tested. One is the insertion with loose clearance and the other is tight clearance of the hole. Following the procedure of the experiment described in the last section, the first function of the vision sensor was successfully performed and the beam was closely aligned with the hole. For the case of loose clearance, no buckling of the beam happened, and the trajectory of the gripper was a piece-wise approximation of the cubic spline function detected by the vision sensor. The insertion of the beam was successfully completed. For the tight clearance case, the vision sensor was used to detect the buckling of the beam once in a while during the insertion process. If the buckling was detected, the manipulator adjusted its court of motion according to the strategy described in [6] and the insertion was also completed smoothly.

VIII. Conclusions

Vision sensors have been successfully used in resolving the uncertainty caused by the deformation of the objects. Several numerical methods have been proposed and analyzed for identifying the deformation characteristic, describing the amount of deformation, and estimating the deformation behavior of one-dimensional objects. These numerical methods have been verified to be effective by experiments.

Although the target of our research in this paper is only one-dimensional objects, we can conclude from this work the procedure for identifying and estimating the deformation of deformable objects as follows.

1. Find out the mathematical equations that describe the deformation of the

objects and determine the deformation characteristics of the objects which are unknown.

2. From the observation of the vision sensor, formulate the approximate mathematical description of the shape of the objects after deformation. By using explicit numerical methods, the deformation characteristics of the objects can be approximately computed.

3. Once the deformation characteristics of the objects have been computed, the numerical methods for estimating the deformation behavior of the objects should be chosen to be robust and efficient in controlling the error. Empirical methods with the aid of the vision sensor can be used to increase the accuracy of the estimation.

IX. References

[1] F. V. Rhode, "Large deflection of cantilever beam with uniformly distributed load," *Quarterly Applied Mathematics*, vol. 11, no. 3, pp. 337-338, 1953.

[2] R. Frisch-Fay, *Flexible Bars*. Washington D.C.: Butter & Co. Limited, 1962.

[3] I. D. Faux and M. J. Pratt, *Computational Geometry for Design and Manufacture*. New York: John Wiley & Sons, 1979.

[4] J. L. Morris, *Computational Methods in Elementary Numerical Analysis*. New York: John Wiley & Sons, 1983.

[5] A. Ralston, *A First Course in Numerical Analysis*. New York: Mcgraw-Hill, 1965.

[6] Yuan. F. Zheng, Run Pei, and Chichyang Chen, "Strategies for automatic assembly of deformable objects." To appear.